iScience

CellPress
OPEN ACCESS

Review

Connecting battery technologies for electric vehicles from battery materials to management

Gang Zhao,[1,*] Xiaolin Wang,[1,*] and Michael Negnevitsky[1]

SUMMARY

Vehicle electrification has always been a hot topic and gradually become a major role in the automobile manufacturing industry over the last two decades. This paper presented comprehensive discussions and insightful evaluations of both conventional electric vehicle (EV) batteries (such as lead-acid, nickel-based, lithium-ion batteries, etc.) and the state-of-the-art battery technologies (such as all-solid-state, silicon-based, lithium-sulphur, metal-air batteries, etc.). Battery major component materials, operating characteristics, theoretical models, manufacturing processes, and end-of-life management were thoroughly reviewed. Different from other reviews focusing on theoretical studies, this review emphasized the key aspects of battery technologies, commercial applications, and lifecycle management. Useful battery managing technologies such as health prediction, charging and discharging, as well as thermal runaway prevention were thoroughly discussed. Two novel hexagon radar charts of all-round evaluations of most reigning and potential EV battery technologies were created to predict the development trend of the EV battery technologies. It showed that lithium-ion batteries (3.9 points) would be still the dominant product for the current commercial EV power battery market in a short term. However, some cutting-edge technologies such as an all-solid-state battery (3.55 points) and silicon-based battery (3.3 points) are highly likely to be the next-generation EV onboard batteries with both higher specific power and better safety performance.

INTRODUCTION

The greenhouse gas (GHG) emission from fossil fuels is regarded as one of the major reasons for climate change and global warming (Hussain et al., 2017). It is estimated that the transportation sector accounts for 14% of the whole fossil fuels GHG emissions in the world (Moustakas et al., 2020). Many countries around the world have made commitments to reduce emissions from their transportation sectors (Lee and Brown, 2021). Replacing conventional internal combustion engine (ICE) vehicles with EVs and hybrid electric vehicles (HEVs) is one of the most effective and practical approaches to reduce GHG emissions (Rao and Wang, 2011). It is reported that a country's GHG emission could be reduced by 40% if all ICE vehicles are shifting to EVs if their charging electricity is purely from renewable sources (Andersen et al., 2009). A rechargeable battery is widely used as the mainstream technology to store energy economically and safely in EVs (Goop et al., 2019). The first rechargeable battery used in automobiles was a lead-acid battery invented by French physicist Gaston Plante in the late 19th century (Jose and Meikandasivam, 2017). In the following century, different types of batteries sprang up such as nickel-based (Ni-based) and lithium-based (Li-based) batteries. In the late 20th century, in the background of the oil crisis and booming energy storage technologies such as lithium-ion (Li-ion) batteries, EV gradually became a dominant part of the automobile industry led by some giant auto original equipment manufacturers (OEMs) such as Tesla, BYD, BMW, Nissan, etc. The large-scale EV productions demand a huge number of reliable and competitive onboard rechargeable energy storage systems. As a result, the safe and reliable battery system became one of the most favorite energy storage options for automobile manufacturers. The battery industry is a highly comprehensive and sophisticated industry composed of mining, chemistry, polymer, metal material as well as electronics industries (Zubi et al., 2018). Global battery production is currently dominated by three major players: China, South Korea, and Japan. The total manufacturing capacity in these three countries reached around 85% of the global Li-ion battery production in 2020 (Placek, 2021). Battery manufacturing companies such as CATL,

[1]School of Engineering, University of Tasmania, Hobart, TAS 7001, Australia

*Correspondence: gang.zhao@utas.edu.au (G.Z.), xiaolin.wang@utas.edu.au (X.W.)

https://doi.org/10.1016/j.isci.2022.103744

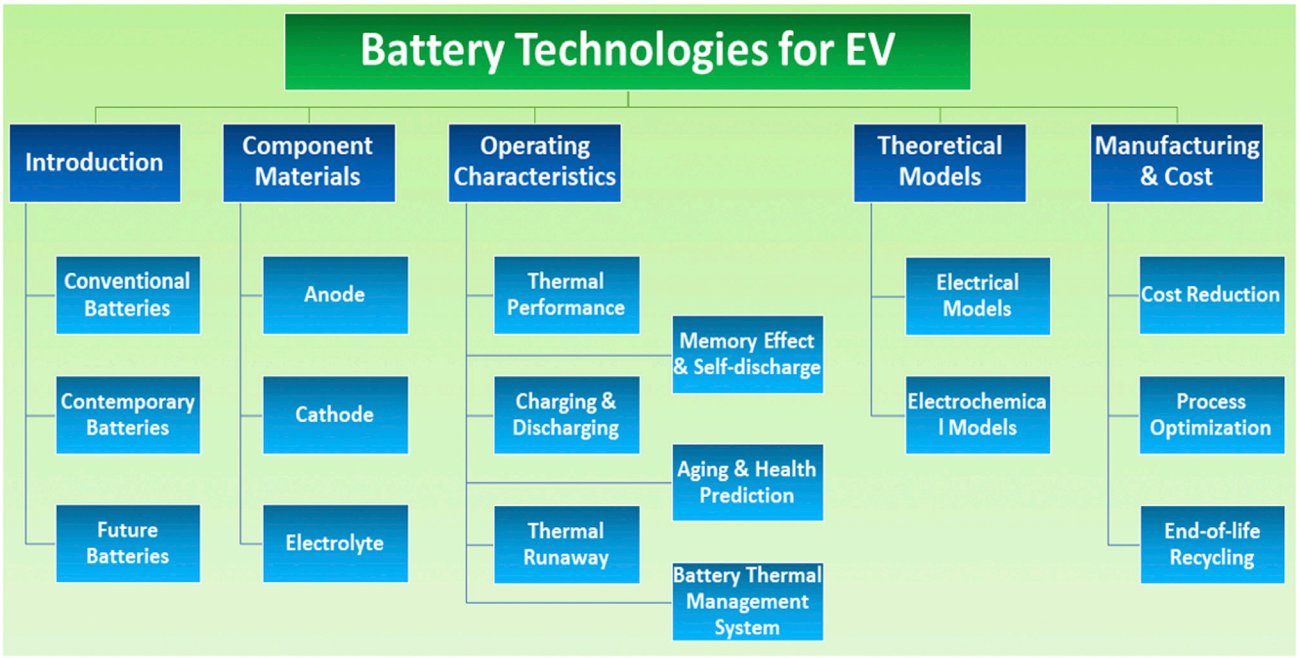

Figure 1. An overview of the contents of this research

Panasonic, LG Chem, Samsung SDI, and SK Innovation had already deployed dozens of Giga factories in Asia, Europe, and North America.

On an average-configured EV, the battery pack is usually the most expensive single component, constituting about 35%–45% of total manufacturing cost. Battery performance influences the overall performance of EVs in terms of power output, driving range, cycle life, safety, etc. However, perfect battery chemistry is not easy to be found. Different anode, cathode, or electrolyte materials exhibit dissimilar pros and cons under various operation conditions. In addition, the raw material prices fluctuate violently due to the unpredictable supply and demand relationships worldwide such as the political unstableness in the Democratic Republic of the Congo (the production place of more than 70% of the world's cobalt) which significantly squeezes the cobalt's supply, environmental devastation by over draining the underground water in South America (more than 60% of the world's lithium reserves are in Peru, Bolivia, Chile, Argentina, etc.) which restricts further mining activities from the giant oversea mining companies, or the novel battery material development which diminishes the cobalt or nickel's constituent percentage in the battery cells. Nonetheless, ideal energy storage chemistries and materials should always be capable of balancing thermal performance and safety as well as delivering satisfied and reliable power output during the whole battery lifecycle.

Figure 1 shows a brief overview of the contents of this research. In this iconic background of the battery era, this article comprehensively reviews the conventional, contemporary, and future battery technologies for commercial EVs to identify the future research directions. Compared with other reviews, the main contribution of this review is detailed below:

- This review connects the battery technologies for EVs from materials to management. The key topics including the development of up-to-date battery component materials, battery operating characteristics, and theoretical models were thoroughly reviewed.
- Critical issues in the battery commercial applications such as advanced health diagnosis, RUL prediction technique, thermal runaway prevention, and battery thermal management system (BTMS) were discussed to find better solutions to extend battery cycle life.
- Battery manufacturing, cost reduction analysis and battery end-of-life recycling were studied to reduce the EV lifecycle costs.

- A perspective of the future EV battery system was discussed.

BATTERIES FOR EV

Lead-acid and Ni-based batteries were the two most commonly used batteries for EVs in the last century (Tie and Tan, 2013). Li-ion battery dominates the current EV battery market. Meanwhile, some promising batteries such as aqueous or solid electrolyte (SE) batteries, Li-O_2 batteries, Li-S battery as well as all-solid-state batteries (ASSBs) are under research and development to be the next-generation EV batteries.

Conventional batteries

In the early 20th century, nearly 30% of the automobiles in the US were driven by lead-acid and Ni-based batteries (Wisniewski, 2010). Lead-acid batteries are widely used as the starting, lighting, and ignition (SLI) batteries for ICE vehicles (Hu et al., 2017). Garche et al. (Garche et al., 2015) adopted a lead-acid battery in a mild hybrid powertrain system (usually no more than 48V) after improving its dynamic charging and discharging performances in 2015. Moseley et al. (Moseley et al., 2012) summarized several performance improvement methods for lead-acid batteries in a high-rate partial state of charge (SoC) operations. Although the upfront capital cost of the deep-cycle lead-acid batteries could reach as low as around 287 $/kWh (Kebede et al., 2021), its cycling performance is not satisfactory due to its low specific energy and short cycle life (Ibrahim et al., 2008). The toxicity of lead could contaminate soil if its disposal was not handled properly (Alkorta et al., 2004). As a result, a lead-acid battery is no longer suitable for the major onboard energy storage device for EVs nowadays. Nickel is lighter than lead and has better electrochemical properties, but the cost of a Ni-based battery is up to 10 times higher than that of the lead-acid one (Hadjipaschalis et al., 2009). Wang et al. (Wang et al., 2012a) developed a novel electrode nickel-iron (Ni-Fe) battery and reached a specific energy value of 120 Wh/kg in 2012. Nickel-cadmium (Ni-Cd) battery was invented in Sweden in 1899. Its specific energy density is lower than that of the nickel-metal hydride (Ni-MH) battery, but its high reliability at low temperatures and low cost are favorite to the EV powertrain system. Owing to the toxicity of Cd, European Union had restricted its usages in the batteries. Ni-MH battery has wide operating temperature ranges and high power density, and it is also environmentally safe by general disposal methods such as landfills (Ovshinsky et al., 1993). Ouyang et al. (Ouyang et al., 2017) suggested that high-energy-density magnesium-based (Mg-based) alloys could be perfect hydrogen storage cathode materials for Ni-MH batteries if their stability in Mg-based electrolyte would be further improved. As the rapid development of Li-ion battery technology in recent years, Ni-based battery's lower specific energy, higher self-discharge rate, and higher heat generation rate at high operating temperatures limit its large-scale commercial applications in the EV industry (Sujitha and Krithiga, 2017).

Contemporary batteries

In 1991, SONY firstly applied Li-ion rechargeable batteries for its commercial electronic products. Its advantages including high specific energy density and power, no memory effect, low self-discharge rate, long calendar life as well as cycle life are all perfect for large-scale commercial productions (Sun et al., 2020b). Figure 2 is a schematic of the electrochemical reaction inside a typical Li-ion battery cell consisting of cathode, anode, and electrolyte. During discharge, lithium ions are released from the anode, traveling through the electrolyte, and intercalated in the cathode. During charging, charged lithium ions are gathered inside the anode after oxidation reactions occurred in the cathode.

The Li-ion battery has been dominating the contemporary onboard EV energy storage device market in recent two decades (Chen et al., 2012). The EV cells are usually categorized into three types: cylindrical, prismatic, and pouch cells (Halimah et al., 2019). The cylindrical cell is a steel shell package of winding electrodes and diaphragm, which is highly suitable for high-speed automatic mass productions. Owing to its high manufacturability and cost-performance, the cylindrical cell is favored by Tesla for almost all its early models. However, the prismatic cell is more beneficial to the battery thermal management due to its cubic shape (Wang et al., 2016). Large surfaces facilitate heat exchange between the cells and cooling media. The regular contour simplifies the design of the air cooling BTMS (Zhao et al., 2021b). As a result, the prismatic cells are widely adopted by large OEMs such as BYD, Volkswagen, Toyota, Nissan, etc. For the pouch cells, although major battery manufacturers such as LG Chem, AESC, and SK Innovation can produce high-quality products, pouch cells are still gradually marginalized over the last few years because of the safety concerns of the frequent accidents due to the cells' swelling and bulging problems (Chen et al., 2021c). Its major customers include GM, Mazda, BAIC, Hyundai, etc.

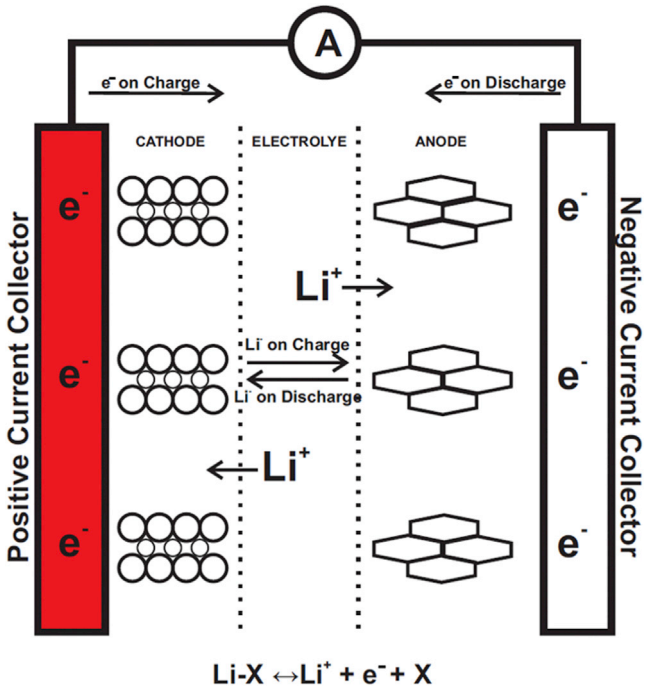

Figure 2. Schematic diagram of a Li-ion battery cell

Li-ion batteries can also be classified by their electrolyte types: liquid-based, polymer-based, and all-solid-state. Most liquid-based electrolytes are aqueous or organic-liquid electrolytes (Miao et al., 2019). They have competitive costs and high technical maturity. But its operating temperature range is narrow, especially at extremely low or high temperatures due to the liquid properties. The polymer-based electrolytes deliver higher specific energy and power (Ceylan et al., 2014; Kim et al., 2008). The heat generation rate of the polymer-based cell increases remarkably during high-rate discharging (Chen and Evans, 1993). Kim et al. (Kim and Lim, 2010) developed better polymer separators at a lower cost, but its overall manufacturing cost is still higher than most of the other Li-ion batteries. Mohammadi (Mohammadi, 2018) successfully installed a 100-kWh Li-ion polymer battery pack on a solar power EV. Some researchers proposed solid biopolymer electrolytes used to obtain higher energy density, higher operating temperatures, and safety performance (Singh et al., 2016). Wegmann et al. (Wegmann et al., 2018) assessed a lithium metal polymer (LMP) high energy battery and proved its wide operation range (up to 80°C). In 2018, LMP battery was commercially used in HEVs for port operations with a wide temperature range from −20°C to 65°C (Zeng et al., 2019b). If the polymer cell could be regarded as a quasi-solid-state battery, the emerging ASSB has the potential to be the next-generation EV battery due to its superior energy density and excellent safety performance. Because it is still under development to be commercially available, it will be introduced in the next section as the future batteries.

Future batteries

The "Future batteries" refer to the novel battery technologies which are currently under development and have the potential to be the next-generation large-scale commercial batteries for EVs such as aqueous-based, Li-ion air (Li-O_2), Li-S, Li-ion silicon (Li-Si), ASSB, zinc-ion (Zn-ion), sodium-ion (Na-ion) batteries, etc. Because the nonaqueous electrolyte is highly flammable and Li-ion salt such as $LiPF_6$ is toxic and unsteady at high temperatures, the non-flammable aqueous electrolyte presents a better safety performance (Hu and Xu, 2014). Aqueous-based Li-ion batteries' excellent reliability and safety features made them appealing for aircraft and submarine uses, which also received attention from the EV engineers to develop them for commercial applications (Ryu et al., 2020). The capacity, energy density, and cycle life of the aqueous Li-ion battery with Li_2SO_4 electrolyte are found to be 100 Ah/kg, 30 Wh/kg, and 1,000 cycles, respectively (Song et al., 2020; Gu et al., 2019). Unlike the low specific energy of the aqueous-based battery, the theoretical specific energy of the Li-ion air (Li-O_2) battery was up to two to three kWh/kg (Black et al.,

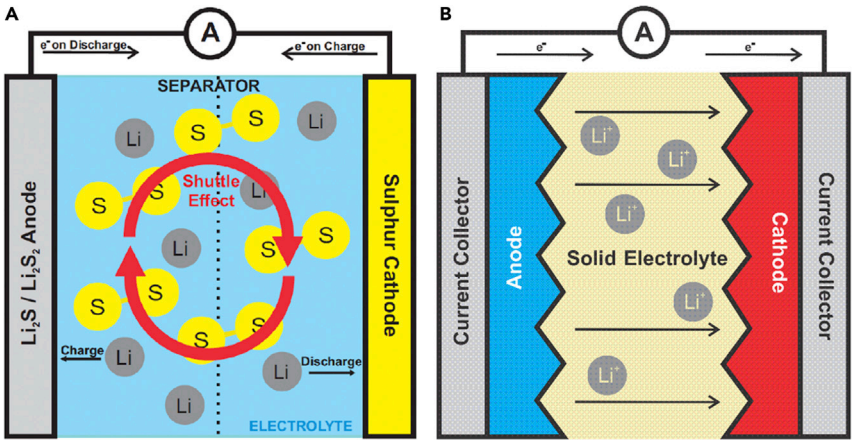

Figure 3. Battery schematic diagrams
(A) Li-S battery (Li et al., 2017e);
(B) Li-ion ASSB (Chen et al., 2021b).

2012). It is a remarkable energy density value at the same level as gasoline, showing the potential to be the "future power source" (Scrosati et al., 2011). However, its charging and discharging efficiencies were urgently needed to be improved by at least two orders larger than the present value to make it more suitable for EV applications (Grande et al., 2015). Additionally, both its low chemical stability and electrical conductivity suppressed its technical maturity (Luntz et al., 2014). Meng et al. (Meng et al., 2021) developed another high-performance rechargeable metal-air battery, Zn-Air battery, delivering a stunning 210-mW/cm^2 high peak power density as well as outstanding cycling stability. With a similar theoretical specific energy of more than 2,500 Wh/kg, the Li-S battery is also a competitive candidate for the next-generation energy storage device. A schematic diagram of the Li-S battery is shown in Figure 3A. Fotouhi et al. (Fotouhi et al., 2016) expected the Li-S battery's bright future due to its higher energy density, better safety performance, broader operation temperature window, and lower manufacturing cost due to the mass-abundance of S in the Earth's crust. The major technical obstacle was the passivation of lithium anode by its reaction with insoluble particles of Li_2S, leading to a high self-discharge rate and fast capacity degradation (Samaniego et al., 2017). Owing to the current technical immaturity, the theoretical specific energy advantage of the Li-S battery was compromised by its poor cycling efficiency and shorter lifetime (Peters et al., 2017). Li-Si battery was another kind of Li-ion battery famous for its theoretical anode capacity of about 4,200 Ah/kg, which is about 10 times higher than some commercial Li-ion battery graphite anodes (Luo et al., 2017). Although the fabrication of high-performance nanostructured silicon materials was expensive and unstable, progress was being made to achieve commercially viable large-scale productions by the coating nanotechnology and manufacturing processes engineering (Li et al., 2018a). Liu et al. (Liu et al., 2019b) coated a second carbon layer on the surface of the silicon nanoparticles encapsulated electrospun carbon nanofibers by pyrolysis method. The novel silicon-based (Si-based) anode material delivered a higher specific capacity of 936.1 Ah/kg during the first discharging cycle and 753.5 Ah/kg during the 100th discharging cycle than that of the one without the second carbon coating.

In recent years, Li-ion ASSB is becoming a hot topic and potential game-changer in the EV industry due to its extraordinary energy density and safety properties. A schematic diagram of the ASSB is shown in Figure 3B. Tan et al. (Shi et al., 2020) adopted a mixing and pressing method to increase the ratio of cathode particle size to the SE particle size to obtain higher cathode loading. Both the simulation and experiment results showed that enlarging the cathode particle size as well as reducing the electrolyte particle size could effectively achieve better utilization of the cathodes. Chen et al. (Chen et al., 2020) used methods of heat treatment and electrospinning to synthesize Ca-CeO_2 nanotubes and sufficient oxygen vacancies in the Ca–CeO_2/LiTFSI/PEO composite electrolyte to obtain higher ionic conductivity and wider electrochemical window than those of the LiTFSI/PEO electrolyte. The results showed that the interactions between nanotubes and LiTFSI could help to tackle the common ASSB problems of low ionic conductivity and few interface contacts. Yamauchi et al. (Yamauchi et al., 2020) improved the rate performances of an oxide ASSB consisting of $Na_2FeP_2O_7$ (NFP) glass and β″-alumina SE by reducing the precursor glass powder particle sizes to enhance the NFP crystallization. The results showed that the novel approach could effectively form the ion conduction

paths within the electrodes and decrease the internal resistance of oxide ASSBs. Ates et al. (Ates et al., 2019) adopted a polyoleophine binder, β-Li_3PS_4, $Li_{1+x}[Ni_{0.6}Mn_{0.2}Co_{0.2}]_{1-x}O_2$, and carbon to produce a composite cathode by tape casting procedure. The dual-electrolyte ASSB exhibited good cycle performance, high specific energy, as well as the potential of scalable productions. As a cheaper and more abundant substitution, the lithium, the sodium-based (Na-based) ASSB (especially the sodium sulfur battery) is expected to be a "future battery" due to its high theoretical specific energy and material earth-abundancy (Wei et al., 2016). Low conductivity and high expansion of sulfur cathodes were the main obstacles to its further applications (Yang et al., 2019). Zhang et al. (Zhang et al., 2020a) intrinsically changed the reaction pathway of sulfur-based (S-based) cathodes with special redox activities to slow down their degradations and reached an energy density of over 1,400 Wh/kg with a durable cycling performance at room temperature. It was also considered as one of the largest energy storage systems (Poullikkas, 2013). Many OEMs have already put some eggs in the basket of ASSBs (Bindra, 2020): Volkswagen invested US$100 million in an ASSB start-up "QuantumScape" from California while Ford, BMW, and Hyundai are the co-investors of a similar SSB developer "Solid Power", ambitiously aiming to deliver the commercially available EV SSBs by 2022. The successful commercialization of ASSBs would significantly increase the driving mileage, simplify the BTMS due to its single-piece large plate structure, and improve the safety with lower heat generation rate.

Finally, as the potential cheaper and safer substitutions of Li-ion batteries, Zn-ion and Na-ion batteries are becoming hot topics for economic EV models recently due to the raw materials' high abundance in Earth's crust, low production costs, superior safety, as well as eco-friendliness (Ming et al., 2019; Deng et al., 2018; Vaalma et al., 2018). Zhang et al. (Zhang et al., 2020b) designed a chemically self-charging aqueous Zn-ion battery with a $CaV_6O_{16}\cdot 3H_2O$ cathode, displaying 1.05V open-circuit voltage (OCV) and 239Ah/kg specific energy during discharging. Xia et al. (Xia et al., 2018) developed an aqueous Zn-ion battery with a novel porous crystal cathode with zinc pyrovanadate ($Zn_3V_2O_7(OH)_2\cdot 2H_2O$) nanowires to achieve specific energy of 214 Wh/kg and 300 cycling stability. He et al. (He et al., 2017) also developed an aqueous Zn-ion battery with an $H_2V_3O_8$ nanowire cathode, zinc anode, and $Zn(CF_3SO_3)_2$ aqueous electrolyte, exhibiting 432.8Ah/kg specific energy and over 1,000 cycling stability. Zhou et al. (Zhou et al., 2017) presented a Na-ion ASSB with a metallic Na anode and ceramic Na superionic conductor (NASICON) electrolyte. The resistance on the Na/ceramic interface was greatly reduced and the dendrite formation was successfully suppressed by the wetting treatment of the electrolyte and the novel sandwich structure of polymer/NASICON/polymer. The Na-ion battery will be playing an important role when the price of lithium keeps going up and safer Na-ion electrolyte is available in the future (Li and Passerini, 2021).

DEVELOPMENT OF ANODE, CATHODE, AND ELECTROLYTE MATERIALS

Electrodes and electrolytes are the most crucial components of batteries. Graphite-based (C-based) metal materials such as graphite-$LiMO_2$ (LMO) are usually used as the substitutions of pure metal anodes. Graphite-$LiMO_2$ batteries are commonly used in portable electronic devices (Etacheri et al., 2011). Other less common lithium-metal based anode materials are Li-TiS_2, Li-MoS_2, and Li-Li_xMnO_2 (Abraham et al., 1989; Dan et al., 1995). Li et al. (Li et al., 2011) discovered a composite of tin (Sn), cobalt (Co), and C as potential anode material. $Li_4Ti_5O_{12}$ (LTO) had lower capacity and energy density, but it could be used in some special applications such as extremely long cycling at low temperatures (Markovsky et al., 2010). Yuan et al. (Yuan et al., 2010) proved that carbon-coated $Li_4Ti_5O_{12}$ anode could improve Li-ion insertion and extraction capacity during high current galvanostatic charging or discharging at a low temperature of −20°C. For the LI-S batteries, an ideal 2D heterostructure anode material of a unique 4-electron transfer per unit feature, molybdenum disulphide (MoS_2), delivered almost three times the theoretical capacity of a graphite anode, but its low intrinsic electric conductivity and stability constrained its wider applications (Xu et al., 2017). Chen et al. (Chen et al., 2016) synthesized porous MoS_2 nanotubes from ultrathin carbon nanosheet structures to stimulate electrochemical reactions. The novel carbon-nanotube-wired MoS_2 tubular structures offered excellent specific capacity of about 1,320 Ah/kg, high-rate capability, and long cycle life.

Si-based material is another option as the ideal anode material for Li-ion batteries owing to its high capacity and Earth's crust abundance (Luo et al., 2017). Liu et al. (Liu et al., 2019c) categorized the SiO-based anode materials into four major types: SiO-based, SiO_2-based, non-stoichiometric SiO_x-based, and Si-*O*-C-based anode materials. Chen et al. (Chen et al., 2019b) reported a Li_xSi anode plating with lithium ions which could prohibit dead Li formation on Li_xSi and enhance the Coulombic efficiency of Li plating/stripping over 99.7%. Iwamura et al. (Iwamura et al., 2015) demonstrated that Li-Si alloy could be a

promising anode material for high-capacity Li-ion batteries in the future. Guan et al. (Guan et al., 2018) fabricated a novel yolk-shell structure porous silicon and carbon (Psi/C) composite anode material for Li-ion battery by methods of spray drying and pyrolysis treatments. This Psi/C-based anode material exhibited a high specific capacity of 1357.43 Ah/kg and high cycling stability of 933.62 Ah/kg after 100 cycles. Yu et al. (Yu et al., 2019) introduced a silicon carbide layer between the carbon layer and the silicon layer to suppress the undesired reaction between silicon and lithium hexafluorophosphate. The aggregation of the reaction products, lithium hexafluorosilicate, was effectively slowed down due to the increase of the activation energy. Cui et al. (Cui et al., 2019) constructed a low-cost Si-based anode material with a controlled mesoporous/microporous structure by the vacuum adsorption method. The cycle stability and electrochemical property of the novel anode material were effectively improved according to the experimental results.

Lithium transition metal oxide cathode materials such as $LiMO_2$, $LiMPO_4$, $LiCoO_2$ (LCO), and $LiNiO_2$ were the early cathode materials (Etacheri et al., 2011). Lithium nickel-cobalt-aluminium oxide ($LiNi_{0.8}Co_{0.15}Al_{0.05}O_2$, NCA) and lithium nickel-manganese-cobalt oxide ($LiNn_{1/3}Mi_{1/3}Co_{1/3}O_2$, NMC) batteries could be regarded as the upgraded versions of $LiMO_2$, i.e., the second generation cathode materials (Majumder et al., 2006; Xiao et al., 2010). Many researchers (Singhal et al., 2006; Kitamura et al., 2011) focused on $LiMn_{1.5}Ni_{0.5}O_4$ cathode material to pursue excellent thermal performance at elevated temperatures with low capacity fading. Li_2MnO_3-$LiMn_{1/3}Ni_{1/3}Co_{1/3}O_2$ was another novel cathode material that could deliver high capacities (>250 mAh g^{-1}) at high voltages and temperatures with low capacity degradation and heat generation rates (Johnson et al., 2004; Lim et al., 2009). Aging research was conducted for NMC-cathode/carbon-anode Li-ion battery cycling at high temperatures (85°C) (Bodenes et al., 2012). The formations of the solid electrolyte interphase (SEI) and the passivation layer on the anodes were thicker at 85°C than those at 60°C.

Except for NCA and NMC batteries, lithium iron phosphate ($LiFePO_4$, LFP) battery is another popular Li-ion battery for EVs. LFP was first explored as commercial cathode material in the late 1990s (Padhi et al., 1997). It delivers high practical capacity and excellent rate capability at low temperatures (Kang and Ceder, 2009; Yaakov et al., 2010). Wu et al. (Wu et al., 2013) designed an LFP cathode using amorphous carbon coating and graphitized carbon coating, exhibiting excellent high-rate capability, excellent cycling capacity retention, and extraordinary low-temperature performance. LFP was less thermally active with common electrolytes than lithiated transition metal oxide cathode materials (Liu et al., 2009). Owing to the success of LFP, $LiMn_{0.8}Fe_{0.2}PO_4$ was developed as an improved cathode material for higher stability in the electrolyte at elevated temperatures as well as better cycling and safety features (Martha et al., 2009; Zhang et al., 2002c). Liao et al. (Liao et al., 2013) added fluoroethylene carbonate (FEC) into the LFP cathode to improve low-temperature performance. They found that the mixed material exhibited higher discharging capacity and better rate performance at low temperatures. R-Mg-Ni-based alloys have been developed as promising cathode materials due to their high hydrogen desorption rate and high energy and power density (Liu et al., 2011). Chen et al. (Chen et al., 2021a) innovatively designed a metal-free cathode catalyst for the reversible conversion and decomposition of Li_2CO_3 for the Li-CO_2 batteries. The novel Li-CO_2 battery is a creative approach to tackle the GHG emission issues.

Alkyl carbonates were applied as the favorite solvent for Li-ion batteries three decades ago (Guyomard and Tarascon, 1992). Several binary solvents were discovered as excellent electrolyte solutions for Li-ion batteries such as ethylene carbonate (EC)-diethyl carbonate (DEC)/ethyl methyl carbonate (EMC)/dimethyl carbonate (DMC) and lithium salt/lithium hexafluorophosphate ($LiPF_6$) (Guyomard and Tarascon, 1992; Tarascon et al., 1994). Ratnakumar et al. (Ratnakumar et al., 2001) explored the effects of SEI on lithium intercalations in a ternary carbonate mixture electrolyte of EC, DMC, and DEC compared with a binary mixture electrolyte of EC and DMC/DEC. EC-DMC/$LiPF_6$ presented high ionic conductivity above −15°C because $LiPF_6$ was highly soluble in most alkyl carbonate solvents. Some advanced active additives such as lithium-bis-oxalato-borate (LiBOB, $LiBC_4O_8$), vinylene carbonate (VC), propargyl-methylsulfone (PMS), HF/H_2O scavengers, and biphenyl or other aromatic molecules had been presented in electrolyte solutions to the moderate surface chemistry of graphite anodes (Verma et al., 2010; Xu, 2004; Zhang, 2006; Shim et al., 2007). Zhang et al. (Zhang et al., 2002a) proved that adding propylene carbonate (PC) into electrolytes could significantly strengthen low-temperature performance by increasing the conductivity of SEI film between electrodes and electrolyte. Some novel materials or structures such as gel (Song et al., 1999), polymetric (Stephan, 2006), and glassy matrices (Parker, 2001) emerged recently as the electrolytes

of solid Li-ion batteries to improve electrochemical and safety performance (Markevich et al., 2008). Herreyre et al. (Herreyre et al., 2001) tested specific ternary mixture electrolytes of cyclic carbonate, linear carbonate solvents, and esters. The novel electrolyte demonstrated excellent thermal performance below −30°C. Zeng et al. (Zeng et al., 2019a) proposed a high salt-to-solvent ratio electrolyte combining fluoroethylene carbonate and di-2,2,2-trifluoroethyl carbonate non-flammable mixture solvent for Si-based anode Li-ion batteries. The novel electrolyte exhibited both high cycling stability and good safety performance. Yang et al. (Yang et al., 2021a) reported a solvation-structure ester electrolyte to establish new dissociation-recombination equilibrium and increase the $LiNO_3$ dissolution levels. With the improved solubility of the $LiNO_3$ in the electrolyte, the anode stability of the lithium metal battery also increased, leading to higher Coulombic efficiency and longer cycle life. Wan et al. (Wan et al., 2019) developed an ASSB with a composite SE combining polyethylene oxide matrix and $Li_7La_3Zr_2O_{12}$ nanowires. The novel battery delivered high ionic conductivity through the electrolyte and low interfacial resistance between electrodes and electrolytes. Gong et al. (Gong et al., 2017) constructed a Li-ion ASSB with $Li_{6.75}La_{2.84}Y_{0.16}Zr_{1.75}Ta_{0.25}O_{12}$ (LLZO) electrolyte and observed its electrochemical delithiation processes from an electron microscope by focused ion beam milling method. The novel *in situ* microscale observation methods will be beneficial for better ASSB designs and improvements. Fan et al. (Fan et al., 2020) designed and fabricated a composite electrolyte combining polyethylene oxide matrix and $Li_{6.75}La_3Zr_{1.75}Ta_{0.25}O_{12}$ nanofibers. The ASSB exhibited excellent ionic conductivity, interface compatibility, and cycling stability at room temperature (25°C).

Table 1 reviews recent research about different types of batteries and their anodes, cathodes, and electrolytes. A general comparison of the technical characteristics of different batteries is listed in Table 2. The Li-ion battery is superior in aspects of energy density, power density, cycle life, and technological maturity (Aifantis et al., 2010; Opitz et al., 2017). It is the most popular energy storage device on the current EV market.

One of the most important functions of a battery cell is to store sufficient electrical energy and supply adequate output power when needed (Burke, 2007). For the EV batteries, their weight should be as light as possible to minimize friction and extend the driving mileage. Figure 4 generalizes the specific energy values of some mainstream and future EV batteries. One of the highest theoretical specific energy Li-ion battery cells is the Li-S battery with a value of about 2,500 Wh/kg (Eftekhari, 2018). Lee et al. (Lee et al., 2019) designed a novel-folded Li-O_2 battery cell and reached a complete cell-scale specific energy of about 1,214 Wh/kg, whose theoretical specific energy was 3,458 Wh/kg. The overall performance of a battery cell is the result of the performances of each component as well as the synergy between them. The component material innovation and manufacturing method breakthrough need the global cooperation and hard works of both the EV industry and academic research communities. There is still a long way to go to commercialize the state-of-the-art batteries for the EV industry, but technical progress are being made to reach the ultimate electrochemical energy storage approach. The driving mileage of the EV will surpass its petrol or diesel counterparts soon.

OPERATING CHARACTERISTICS

Thermal performance

The thermal performance of a battery cell refers to its heat generations and output performances at different temperatures. For most batteries, the low temperature would affect their specific energy and power (Nagasubramanian, 2001), charge acceptance (Burow et al., 2016), discharging performance, degradation, cycle life, etc. Zhang et al. (Zhang et al., 2002b) found that graphite anode capacity decreased dramatically from 0°C to −20°C. Waldmann et al. (Waldmann et al., 2014) investigated the relationship between aging rate and temperatures from −20°C to 70°C: operations at 25°C exhibited the lowest battery aging rate and −20°C was more detrimental to the battery than 70°C in terms of aging behavior. To accelerate the Li-ion solvation sheath evolution and remote lithium dendrite formation at low temperatures, Wang et al. (Wang et al., 2021) regulated the fluorination degree of solvating agents (including ethylene carbonate-based fluorinated derivatives, difluoroethylene carbonate, fluoroethylene carbonate, etc.) via an ion-dipole strategy. The novel electrolyte showed a six times higher ion desolation rate than the non-fluorinated electrolyte at −20°C. Huang et al. (Huang et al., 2000) discovered that low diffusivity and limited capacity on the carbon anodes under −30°C were the main factors of Li-ion battery poor thermal performance at low temperatures. Lin et al. (Lin et al., 2001) found that polarization of carbon anodes under −20°C were the main cause of the battery permanent capacity loss. Liao et al. (Liao et al., 2012) also found

Table 1. Different types of batteries and their anodes, cathodes, and electrolytes

Battery	Anode (+)	Cathode (−)	Electrolyte	References
Lead-acid	Lead Dioxide (PbO_2)	Sponge lead (Pb)	Sulfuric acid (H_2SO_4)	Conte, 2006; Bukhari et al., 2015
Lead crystal	Lead Dioxide (PbO_2)	Spongy lead (Pb)	Composite SiO_2 electrolyte	Bukhari et al., 2015
Ni-Cd	NiOOH and $Ni(OH)_2$	Cadmium (Cd)	Alkaline electrolyte (commonly KOH)	Karkera et al., 2021
Ni-MH	Nickel oxyhydroxide (NiOOH)	Hydrogen ions or protons (MH)	Alkaline electrolyte (usually KOH)	Du, 2017
LG MJ1	Graphite	$Ni_{0.81}Co_{0.13}Mn_{0.06}$	Ethylene carbonate (EC), diethyl carbonate (DMC), $LiPF_6$, LiFSI	Krause et al., 2019
SA35E-10	Graphite	$Ni_{0.83}Co_{0.15}Al_{0.02}$	EC, DMC, additive, $LiPF_6$, LiFSI	
PBJ-10	Graphite	$Ni_{0.81}Co_{0.16}Al_{0.04}$	EC, DMC (assumed), $LiPF_6$, LiFSI	
LM36-10	Graphite	$Ni_{0.86}Co_{0.12}Al_{0.02}$ and $LiMn_2O_4$	EC, DMC, $LiPF_6$, LiFSI	
SOVC7-10	Graphite	$Ni_{0.90}Co_{0.08}Al_{0.02}$	EC, DMC, $LiPF_6$, LiFSI	
Li-NCA	Graphite	NA	1 M $LiPF_6$ in 1:1:1 w (weight ratio) EC/DEC/DMC (LP71) (Bertilsson et al., 2017)	Sabet et al., 2018
$LiCoO_2$ (LCO)	Graphite or graphitized carbon fiber	$LiCo_{0.2}Ni_{0.8}O_2$ or Li_xCoO_2	1,1- diphenylmethane with 5 wt% DPE for the full cells (Yatabe et al., 2018)	Al Hallaj et al., 2000
Ge-$LiCoO_2$	Ge	RF-sputtered lithium cobalt oxide ($LiCoO_2$)	Lithium Phosphorus Oxynitride (LiPON)	Vieira et al., 2017
Li-ion Manganese Oxide (LMO)	Graphitized carbon	$Li_{1.1}(Ni_{0.025}Ti_{0.025}Mg_{0.02})Mn_{1.83}O_4$	$LiPF_6$/ethylene carbonate + diethyl carbonate + dimethyl carbonate	Yoshida et al., 2006
Li-NMC	LiC_6 or LiC_{12}	$Li_x(Ni_{0.5}Mn_{0.3}Co_{0.2})O_2$ such as $LiNi_{1/3}Mn_{1/3}Co_{1/3}O_2$	1 M $LiPF_6$ in 3:7 (volume ratio) EC/EMC with additives such as VC, PES, FEC, etc. (Genieser et al., 2018)	Dolotko et al., 2014
LFP	Mesocarbon microbead (MCMB) graphite	Carbon-coated LFP	LFP/EC-DEC	Amine et al., 2005
Li-S	Li	S	Lithium trifluoromethanesulfonate (or lithium triflate) $LiSO_3CF_3$, Lithium bis(trifluoromethanesulfony)amide (or LiTFSA) $LiN(SO_2CF_3)_2$	Samaniego et al., 2017, Yang et al., 2010, Moy et al., 2015, Wei et al., 2021
	Si nanowire	Li_2S nanocomposite/mesoporous carbon	Room temperature ionic liquid (N-methyl-N-butyl-piperidinium bis (trifluoromethanesulfonyl) imide (PP14-RTIL)) (Yuan et al., 2006)	
	Li	S	0.5 M LiTFSI in 1:1 DOL/DME	

(*Continued on next page*)

Table 1. *Continued*

Battery	Anode (+)	Cathode (−)	Electrolyte	References
Li–TiS_2	TiS_2	$LiMn_2O_4$	21 m LiTFSI in H_2O (Water-in Salt electrolyte)	Sun et al., 2017
Li–MoS_2	MoS_2	$LiNi_{0.5}Co_{0.3}Mn_{0.2}O_2$	1m $LiPF_6$ in EC/DMC with 10 wt % FEC	Zhu et al., 2018
Li-Si	Si nanowires (SiNW)	Li	1 M solution of $LiPF_6$ diluted in a mixture of ethylene (EC), dimethyl carbonate (DMC), and diethyl carbonate (DEC) with a 1:1:1 vol ratio	Refino et al., 2021
Li-Sn	Li	Li_xSn	1 M LiPF6 in ethylene carbonate (EC)/propylene carbonate (PC)/ dimethyl carbonate (DMC) (1:1:3 v/v/v)	Ehinon et al., 2008
Li-Se	Li–Sn alloy	Se–Li_3PS_4–C	Li_3PS_4	Li et al., 2018b
$LiBF_4$	Carbon	Lithium metal oxide	$LiBF_4$-based electrolyte	Zhang et al., 2002c
SAFT DD	MCMB-carbon	$LiNi_{0.8}Co_{0.2}O_2$	1.0 M $LiPF_6$ EC + DEC + DMC + EMC (1:1:1:2 v/v); 1.0 M $LiPF_6$ EC + DEC + DMC + EMC (1:1:1:3 v/v)	Smart et al., 2003
Li/Polymer	Li foil	A slurry with 80 wt% of $LiFePO_4$, 10 wt% of Super P (SP), and 10 wt% of polyvinylidene fluoride (PVDF) in 1-methyl-2-pyrrolidone (NMP) casted on Al foils	Gel polymer electrolyte	Yuan et al., 2021
Metal-air	Zn plate	A commercial carbon cloth coated with solid catalyst	An aqueous solution mixture of $6.0molL^{-1}$ KOH-$0.2molL^{-1}$ $(CH_3COO)_2Zn$	Huang et al., 2022
Li-O_2	Li metal chip	Ru/B_4C	1 M LiTFSI in tetraglyme	Song et al., 2019
Na-S	Na or low potential alloys	Synthesized Na_2S-Na_3PS_4-CMK-3 composite	Solid-state $Na_{11}O_{17}$	Fan et al., 2018
Zn-ion	Zinc	$H_2V_3O_8$ nanowire	Zn $(CF_3SO_3)_2$ aqueous electrolyte	He et al., 2017

Table 2. A general comparison of the technical characteristics of different batteries

Category	Energy density	Power density	Nominal voltage	Overcharge tolerance	Self-discharge	Memory effects	Cycle life	Environmental toxicity	Technological maturity	References
Lead-acid	Low	Low	Medium	High	Medium	Very Low	Low	High	High	Berndt, 1997
Lead crystal	Medium	Medium	High	High	Medium	Very Low	High	Low	Medium	Bukhari et al., 2015
Ni-Cd	Low	Low	Low	Medium	Very High	High	High	High	High	Zelinsky et al., 2018
Ni-MH	Medium	Medium	Low	Medium	High	High	Medium	Low	Medium	Ouyang et al., 2017
Lithium-ion	High	High	High	Low	Very Low	Very Low	High	Medium	High	Liu et al., 2021b
Li-air	Very High	Very High	Low	Low	–	–	Low	Low	Low	Xu et al., 2019
Na-S	High	Medium	–	–	Low	–	Medium	Low	Low	Aneke and Wang, 2016
Li-S	Very High	Very High	Medium	Low	Medium	Low	Low	Low	Low	Fu et al., 2021
Li-Si	Very High	Very High	Low	–	–	–	Low	Low	Low	Zhao et al., 2019
ASSB	High	High	High	High	Low	Low	Medium	Low	Medium	Baade and Wood, 2021

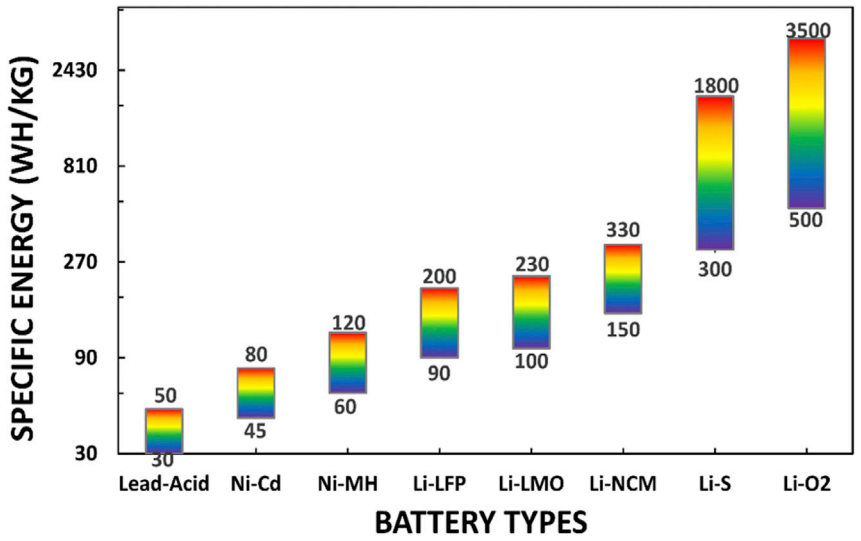

Figure 4. The specific energy values of some mainstream and future EV batteries

that low temperature (−20°C) affected the discharge capacity during discharging more than the charge capacity during charging. During cycling below −10°C, the charge-transfer resistance would be significantly increased, showing the poor thermal performance (Zhang et al., 2003). Battery power (voltage) and energy (capacity) performance were both reduced significantly at low temperatures (Zhang et al., 2004). The minimum performance temperature of some dimethyl carbonate (DMC) electrolyte-based Li-ion batteries was limited to −20°C (Smart et al., 1999). The lithium plating was occurring during charging and discharging at low temperatures and was expedited by higher currents, voltages, and electrode kinetics (Smart et al., 2002). Wu et al. (Wu et al., 2017) discovered that the $LiCoO_2$/$LiNi_{0.8}Co_{0.15}Al_{0.05}O_2$ pouch battery was sensitive to low temperature due to the cathode degradations. Gao et al. (Gao et al., 2002) explored the relationship between temperatures and capacities for Li-ion batteries. At −20°C, both voltages and state of discharges (SoDs) were about 20% lower than those at 45°C. At −40°C, the power density and energy density of Panasonic 18,650 Li-ion batteries were only about 1.25% and 5% of those at 25°C (Nagasubramanian, 2001). Lindgren et al. (Lindgren and Lund, 2016) reported that a Li-ion battery's self-weighted mean charging power (SWMCP) at −10°C could only reach about 85% of that at 20°C. Preheating strategy is a common solution to solve the low-temperature issue. Li et al. (Li et al., 2021c) polarized the cells by pulse currents to provide rapid heating at low temperatures. The novel method was proven to be low cost and almost no influence on the battery degradation.

At high temperatures, more side reactions were triggered at cathodes (Broussely et al., 2005). Electrolyte oxidations increased cell impedance and reduced active surface area, causing aging and short cycle life (Vetter et al., 2005). Shim et al. (Shim et al., 2002) conducted experiments on $LiNi_{0.8}Co_{0.15}Al_{0.05}O_2$/graphite Li-ion pouch batteries and found that decomposition of conductive carbon at cathodes or a film of SEI on the cathode surfaces at 60°C might cause a permanent capacity loss after cycling operations. Santhanagopalan et al. (Santhanagopalan et al., 2008) found that a higher temperature could cause more active material loss. Li et al. (Tan et al., 2013) observed that the high temperature fostered Li inventory loss on graphite anode surfaces during charging and discharging cycles, leading to irreversible capacity fade.

In addition to the extreme temperatures, the temperature difference within a battery cell is another major influential factor to its thermal performance. Robinson et al. (Robinson et al., 2014) observed that the warmest component of a single 18,650 Li-ion cell was the positive terminal around the anode battery cap. Panchal et al. (Panchal et al., 2017) conducted experiments on LFP prismatic batteries at different temperatures and showed that uneven temperature distribution came from different heat generation rates on different parts of the cell: surface and centerline temperatures are always lower than electrode tab temperatures while anode current collector temperature is always higher than cathode current collector temperature. They observed 18,650 cell temperature patterns at discharging

Table 3. Self-discharge performance from different batteries

Battery type	Estimated self-discharge rate	References
Li-ion battery	5% in 24h, then 1%–3% per month (plus 3% for safety circuit)	Swierczynski et al., 2014
Lithium polymer battery	~10% per month	Swierczynski et al., 2014
Lead-acid battery	4%–6% per month	Swierczynski et al., 2014
Ni-Cd battery	10%–15% per month	Jeyaseelan et al., 2020
Ni-MH battery	30% per month	González-Gil et al., 2013
Na-S battery	10%–20% per day	Chatzivasileiadi et al., 2013
Li-S battery	50% in a month or less	Wen et al., 2020
Vanadium redox battery	~2% per month	Swierczynski et al., 2014
Rechargeable alkaline battery	3% per year	Hopkins et al., 2020

rates of 1C, 2C, 3C, and 4C and reported that higher discharging rates led to elevated surface temperatures (Panchal et al., 2018). Wu et al. (Wu et al., 2018) found that the prismatic battery's internal anisotropic characteristics had an influential impact on heat transfer performance. Higher battery thickness led to fewer cross-section temperature distributions. Not only the temperature difference within a single cell but also that among different cells could affect the battery thermal performances. Feng et al. (Feng et al., 2018b) investigated the relationship between charging status variations and inhomogeneous temperature distributions and pointed out that every 5°C increment on the temperature difference could incur 1.5%–2% more capacity loss. Kuper et al. (Kuper et al., 2009) commented that 5°C of temperature difference could cause about 10% capacity degradation. Iraola et al. (Iraola et al., 2014) proposed a novel voltage balancing strategy to improve temperature gradient performances and minimize aging during deep discharging cycling.

Memory effect and self-discharge

Memory effect reduces battery cycle life by remembering the previous charging status if the previous one is not fully charged (Suberu et al., 2014). Memory effect is mainly observed in Ni-Cd and Ni-MH rechargeable batteries (Bergveld et al., 2002). The repeated partial discharging or charging might cause a decrease in rated energy capacity. Sato et al. (Sato et al., 2001) studied commercial AAA Ni-Cd as well as Ni-MH batteries by X-ray diffraction analysis and concluded that the main cause of the memory effect was the formation and accumulation of γ-NiOOH formed at the electrodes during repeated shallow discharging or overcharging. Gao et al. (Gao et al., 2012) presented a novel $Cd(OH)_2$ nanowire anode for Ni-Cd battery to improve capacity and eliminate the memory effect. The new anode reduced about 80% of the pollution of toxic Cd released to the environment. On the other hand, lead-acid and Li-ion batteries were generally regarded as ideal energy storage devices in terms of nearly no memory effect. However, Nelson et al. (Nelson and Wisdom, 1991) observed a phenomenon similar to a memory effect in lead-acid batteries that some passivation layers would be built upon the anodes during deep cycling operations, losing battery capacity. Sasaki et al. (Sasaki et al., 2013) reported a memory effect that appeared in the anode of the LFP battery only after one cycle of partial charging and discharging. Ulldemolins et al. (Ulldemolins et al., 2013) revealed a memory effect that happened on Si anodes of high energy density Li-Si batteries in the lithium insertion/desertion processes when the cut-off voltage was less than or equal to 50 mV during discharging.

As another common adverse phenomenon to the batteries, the self-discharge leads to the unwanted depletion of stored energy without doing any useful work (Garche et al., 2013). The thermodynamical stability in a fully charged state is always lower than that in a partial or fully discharged state, so the battery intrinsically tends to return to a lower potential energy status by turning into a discharged state. Thermal equilibrium is gradually achieved by self-discharge (Sloop et al., 2003). Different batteries and chemistries exhibit different self-discharge rates as detailed in Table 3.

The average self-discharge rate for Ni-Cd batteries is about 15%–20% per month (Dyer et al., 2009). Senthilkumar et al. (Senthilkumar et al., 2017) explained the high self-discharge rate of Ni-Cd battery which was caused by the instability of fully charged anodes. For the Ni-MH B2 battery, Zhu et al. (Zhu et al., 2013)

found its remaining capacity of about 70% of the full value after 1,519-h storage self-discharge. Feng et al. (Feng and Northwood, 2005) stated that the main cause of Ni-MH self-discharge was a decrease in the hydrogen storage or increase in hydrogen diffusion rate on the MH anodes. Leblanc et al. (Leblanc et al., 1998) used a specially designed grafted polyolefin separator to slow down the decompositions of active materials on the anodes to reduce the self-discharge rate.

Li-ion and lead-acid batteries demonstrated lower self-discharge characteristics than Ni-based batteries. Lead-acid battery self-discharge was usually influenced by ambient temperature, state of health (SoH), and SoC (Gell, 2013). Bullock et al. (Bullock and Laird, 1982) found that the lead-acid battery in an acid-starved state had a lower self-discharge rate than that in a fully flooded condition. Seong et al. (Seong et al., 2018) found that a quick thermal exposure would abnormally accelerate battery self-discharge. Zimmerman (Zimmerman, 2012) measured self-discharge losses in Li-ion batteries and found that the losses were mainly influenced by time and SoC, but most self-discharge losses were very low. On the other hand, Li-S batteries exhibit serious self-discharging problems as well as poor cycling stability (Li et al., 2017d). Resting the Li-S battery at both higher and lower voltage plateaus would cause more rapid self-discharging. The suggested storing voltage is about 2.10V (Wen et al., 2020). Ryu et al. (Ryu et al., 2006) used tetra ethylene glycol dimethylether in the Li-S battery electrolyte with an Aluminum current collector to reduce the self-discharge rate. The research team (Ryu et al., 2005) also adopted a gold-coated current collector to reduce self-discharge because it had better anti-corrosion property.

Charging and discharging

As an important indicator of the battery status, SoC describes the charging status and remaining discharging capacity (Chiang et al., 2011). SoC estimation via the measurements of cell voltage, pack current, and temperature is an important function of the EV battery management system (BMS) (Gabbar et al., 2021). Ramadass et al. (Ramadass et al., 2003) discovered the correlation between the SoC and the active material loss. Li et al. (Li et al., 2016a) found that SoC was an indicator of battery real capacity. Accurate SoC monitoring and prediction is crucial to a successful BMS (Li et al., 2019b). Pang et al. (Pang et al., 2001) presented a novel algorithm to estimate the SoC as well as its optimal range for better battery performance. Bhangu et al. (Bhangu et al., 2005) proposed a state-estimation methodology for real-time prediction of lead-acid battery SoC, demonstrating an error of less than 2%. Chiasson et al. (Chiasson and Vairamohan, 2003) designed an electric circuit model to describe the relationship between SoC and OCV. Chen et al. (Chen et al., 2019d) used the reconstructed OCV curve to obtain more accurate SoC estimations. Different cycling SoCs imposed different levels of impacts on battery degradation and aging at different charging temperatures. Li et al. (Li et al., 2017a) controlled the battery SoC status adaptively by real-time vehicle control parameters to acquire optimal fuel economy. Meng et al. (Meng et al., 2018) created a Ni-MH BMS by containing the battery SoC status within the optimal operation window through precise online measurements and modifications. Hannan et al. (Hannan et al., 2017) concluded that an accurate methodology of estimating Li-ion battery's SoC would dominate the future EV market. Recently, Wang et al. (Wang et al., 2020b) improved an iterate calculation method to predict the SoC of the lithium-ion battery (LIB) packs more accurate by a novel splice Kalman filtering algorithm with adaptive robust modeling and noise correction, delivering a basic SoC prediction approach for LIB packs. The Ni-based battery could only be partially charged while a Li-ion battery would suffer from severe degradation and aging at high temperatures. Gonzalez et al. (Gonzalez et al., 1996) presented an optimized fast charging strategy for Ni-Cd and Ni-MH batteries: collecting battery status parameters (SoC, SoH, etc.) to real-time control charging time. Nazari et al. (Nazari et al., 2018) studied LFPs with different nominal capacities at different charging/discharging rates and calculated the overall heat generation rates as well as charging/discharging efficiencies. Li-Ti battery was regarded as a promising battery due to its excellent fast charging capability (Low et al., 2016). During normal EV operations, the average charging and discharging rates are moderate. In the world harmonized light-duty vehicles test procedure (WLTP) (Hooftman et al., 2018), the average speeds without stops for low-power vehicles (power/weight ratio $\leq$22 W/kg), vehicles (22 W/kg< power/weight ratio $\leq$34 W/kg), and high-power vehicles (power/weight ratio >34 W/kg) are 35.6 km/h, 42.4 km/h, and 53.5 km/h, respectively. If the average discharging time for the EV batteries from 100% SoC to the cut-off voltage is about 5 h, the average discharging C-rate will be 0.2C. The fast charging station is generally required to deliver a charging capability of replenishing the 60-mile (97 km) range in 10–30 min. SAE international defines Level 3 charging as supercharging: 80% of total capacity within 30 min. The fastest Direct Current charging could provide a 100 km range within 10 min via charging power of 120 kW. Its voltage range is 300–500 V and the current range is 300–350 A. Higher charging rates correspondingly lead to higher heat generation. If the excessive heat could not be dissipated efficiently, the battery temperature would rise to a harmful level to the battery system.

However, in some special cases such as fast charging and abusive discharging, the heat generation rates will be intense. Suitable fast charging ambient temperatures of most Li-ion batteries should be controlled around 25°C. Lu et al. (Lu et al., 2019) found that the charging performance showed good consistency in a favored range of 20°C–40°C. The charging/discharging performances decreased significantly below 20°C. They also discovered that the proper battery self-heating during moderate discharging would improve output performance, indicating that the favorable discharging temperatures could be higher than charging ones. Roth et al. (Roth et al., 2004) explored the Li-ion battery abuse discharging mechanisms in the anode and cathode reactions. Internal heat was generated from energy loss during discharging (Thomas and Newman, 2003). When the battery was unintentionally shorted or intentionally abused such as racing and abusive driving, the soaring temperature would influence its thermal and safety performance. In the worst external short case, the 16P 18,650 would generate 20-W heat hazardously if it sustained (Smith et al., 2010). Liu et al. (Liu et al., 2014) found that fast and deep discharging would yield over temperatures regardless of cooling conditions. Excessive waste heat would be generated by large currents due to battery internal chemistry and ohmic resistance (Giuliano et al., 2011). Lin et al. (Lin et al., 2012) defined 8C as rapid acceleration and 10C as drastic braking. Batteries with active materials such as Ni, Mg, or phosphate could tolerate up to 10C discharging. Wang et al. (Wang et al., 2015) observed that the maximum LFP battery surface temperature reached around 76.5°Cat 35A discharging current and the electrodes behaved more active than other components at high temperatures.

Aging and health prediction

The cycle life of most rechargeable batteries is majorly affected by galvanostatic charging or discharging processes (Li et al., 2021a). Barré et al. (Barré et al., 2013) categorized battery aging into two types: calendar aging and cycle aging. The calendar aging usually happens during storage and cycle one occurs during periodical charging and discharging. Yoshida et al. (Yoshida et al., 2003) used a simple formula to predict calendar capacity loss by multiplying the calendar capacity loss coefficient and the square root of storage time. Mukhopadhyay et al. (Mukhopadhyay and Sheldon, 2014) highlighted that cycling mechanical stresses and deformations from vehicle dynamic motions might cause surface destructions between electrodes and electrolytes, leading to capacity fade and aging. Adams et al. (Adams et al., 2018) evaluated the mechanical shock impacts on battery aging and degradation. The results showed that cycling dynamic impacts would increase the residual stresses on the electrode interfaces and decrease battery Coulombic and energy efficiency, causing $LiCoO_2$ cathode degradations. Temperature is the dominant factor in both calendar and cycle aging (Bögel et al., 1998; Nunotani et al., 2011). Wright et al. (Wright et al., 2003) tested 18,650 cells at 45°C and displayed a faster capacity fade rate proportional to the square root of total cycling time compared with a slower linear fade rate at 25°C. As the cycling number increases, degradations would be more rapid with rising temperature (>40°C) while capacity would decrease contrarily with higher temperature (Lindgren and Lund, 2016). Waldmann et al. (Waldmann et al., 2014) discovered that 25°C was the optimal temperature for a longer cycle life of $Li_xNi_{1/3}Mn_{1/3}Co_{1/3}O_2/Li_yMn_2O_4$ blended cathode-graphite/carbon 18,650 battery. The degradation and capacity fading phenomenon was most obvious during storage and operation at 60°C–90°C (Bodenes et al., 2012). Higher temperatures tended to accelerate SEI formation while lower temperatures fostered lithium plating as well as cathode degradation during the final charging period, both causing capacity fade and degradation (Wu et al., 2017). They also found that pouch cell designs had the advantages of receiving less cycling mechanical and thermal stresses during high C-rate discharging, which was beneficial to resist aging and degradation during fast discharging. Nunotani et al. (Nunotani et al., 2011) speculated that the reason for faster cycle aging rate at low temperature (5°C) was that the binder flexibility decreased more rapidly at low temperature during repeated expansions and contractions. Table 4 lists the capacity fade rates of several EV batteries at different cycling charging/discharging rates, number of cycles, and temperatures. The battery capacity fade rates are primarily proportional to the charging/discharging rates and operation temperatures.

Internal resistance is a crucial parameter to precisely predict the SoH of the battery (Sun et al., 2020a). Its value is usually high at low temperature or in extreme SoC status close to either 0% or 100%. John et al. (Hall et al., 2006) discovered that the internal resistance growth was related to the end-of-charge voltage. Irreversible reactions would result in an increase in internal resistance and a decrease in maximum capacity (Xiong, 2020). Some other factors such as manufacturing, transportation, and storage might affect internal resistance (Gogoana, 2012; Barai et al., 2017). Stroe et al. (Stroe et al., 2016) found that LFP internal resistance increased with storage time following a non-linear power-law function. Ye et al. (Ye et al., 2014) suggested mixing thermal conductive materials or shrinking particle sizes of active materials to decrease

Table 4. The capacity fade rates of several EV batteries during different cycling charging/discharging operations

Batterytype	Charging/ discharging rate	Number of cycles	Temperature (°C)	Capacity fade rate (%)	References
Sony 18,650 Li-ion battery	–	800	45	36	Ramadass et al., 2002
		490	55	70	
$LiNi_{0.8}Co_{0.15}Al_{0.05}O_2$/ graphite Li-ion pouch battery	0.5C	140	25	4	Shim et al., 2002
			60	65	
LFP battery	0.33C	100	37	55	Amine et al., 2005
			55	72	
	0.5C	2,628	15	7.5	Liu et al., 2010
	0.5C	757	60	20.1	
	6C	1,376	45	22.1	
	1C	5,000	35	21	Millner, 2010
		1,500	45	18	
$LiFeMnP0_4$ battery	1C	170	25	6.9	Jaguemont et al., 2015
	0.1C	2000	25	20	
	1C	12	−20	20.8	
Commercial LFP/graphite cylindrical battery	0.04C	3,800	23	17	Anseán et al., 2016
LFP/Mesocarbon Microbead (MCMB) battery	0.1C	100	−10	2.97	Zheng et al., 2017
	0.33C			12.77	
	0.5C	40		30.69	
	1C	20		29.33	
LG INR18650HG2	0.5C	67	5	20	Mathieu et al., 2019
		258	25		
		438	45		
SAMSUNG INR1865025R		480	5		
		339	25		
		330	45		
A123 APR18650M1B		7,400	5		
		2,100	25		
		1,551	45		

internal resistance between collectors and active materials. Tan et al. (Tan et al., 2020) found a strong correlation between battery degradation and equivalent internal resistance (EIR) over the whole lifetime. Because the EIR value is more practical and feasible to be measured, the battery cycle life could be predicted by a function of EIR indirectly (Hall et al., 2006). Wei et al. (Wei et al., 2009) set up an index model to estimate battery lifetime from real-time internal ohmic resistance values by adopting a recursive least squares algorithm. Stroe et al. (Stroe et al., 2017) investigated the degradation based on aging experiments and designed an accurate semi-empirical model to predict battery lifetime.

Battery SoH estimation and RUL prediction are beneficial to battery performance, cycle lifespan extension, maintenance, and malfunction or accident prevention (Allam et al., 2020). Xiong et al. (Xiong et al., 2018) divided the battery SoH estimation methods into two types: experimental methods and model-based methods. The experimental methods can be divided into direct measurement methods (measuring the capacity, impedance, or other parameters to indicate the SoH) and indirect analysis methods (analyzing and processing data to predict SoH). The model-based methods can be regarded as an extension of the indirect analysis model methods. Both battery internal resistance and actual energy storage capacity can be used to indicate and predict the battery SoH (Richardson et al., 2019), but the actual capacity is more favored by the research of the SoH predictions for the EV onboard power batteries because the actual capacity could be used to calculate SoH directly (SoH is the ratio of the maximum charge capacity to the battery rated capacity) while the internal resistance is just one of the crucial indicators of the battery SoH. Wei

et al. (Wei et al., 2017) established a support vector regression-based SoH state-space model to simulate the battery aging mechanism by extracting the capacity and representative features as the state variable. Wang et al. (Wang et al., 2017b) designed an accurate discharge-rate-dependent state-space model to track usable battery capacity and predict the RUL affected by different discharge rates. Liu et al. (Liu et al., 2019a) proposed an improved Li-ion battery degradation model based on the capacity fade electrochemical mechanism to forecast both the short-term and long-term degradation. The accuracy and applicability of the method were verified by the battery cycling test datasets with low SoH and RUL root-mean-square errors. Kyungnam et al. (Park et al., 2020) proposed a data-driven long short-term memory-based model to predict the RUL more accurately using a novel many-to-one structure. The novel structure not only captured the capacity regeneration phenomenon but also reduced the parameter numbers. Zhang et al. (Zhang et al., 2017b) proposed an improved Markov chain Monte Carlo-based unscented particle filter method to tackle the sample impoverishment problem in the algorithm. Sun et al. (Sun et al., 2018) incorporated capacitance, resistance, and constant current charge time into an integrated battery health indicator to predict RUL by a beta distribution function. The constant current charge time was found to be a less effective health indicator by the case validations. Li et al. (Li et al., 2019a) firstly developed an inheritance particle filter for an RUL prediction model to effectively tackle the problems of impoverishment deficiency and particle degeneracy. Duong et al. (Duong and Raghavan, 2018) introduced an RUL prediction method combining the Heuristic Kalman algorithm and particle filtering to solve the issue of sample degeneracy and impoverishment. The accuracy of the novel method was proven by NASA datasets. Xu et al. (Xu et al., 2021) proposed a stacked denoising autoencoder method based on a deep learning mechanism to predict battery life from the essential battery features including discharging temperatures and voltage curves filtered by clustering fast search (CFS) method. The model was validated using experimental data and showed more accurate and efficient prediction results than the one without using the CFS method.

Hosen et al. (Hosen et al., 2021) adopted a semi-empirical modeling approach to predict the complex LIB aging phenomenon. The non-linear autoregressive network was proven to be more precise than machine learning and artificial neural network models with minimal computational costs. However, Shu et al. (Shu et al., 2021) were optimistic about the machine-learning-based SoH prediction methods due to their simplicity and accuracy and considered them as game-changers for future transportation electrification. Ren et al. (Ren et al., 2018) proposed a deep learning-based RUL prediction model which extracts features via autoencoder model and estimates remaining cycle life via deep neural network training. Li et al. (Li et al., 2020) proposed a multiple cells data-driven prognostic framework to improve the SoH and RUL predictions using a method of variant long short-term memory neural network. The novel method exhibited lower average root-mean-square and conjunct error values than other data-driven methods. Richardson et al. (Richardson et al., 2019) formed a generalized Gaussian process regression health model to predict battery capacity fade under different operational conditions. NASA open-source Randomized Battery Usage Dataset was adopted to train and validate the model's long-term capacity fade prediction successfully. Lin et al. (Lin et al., 2020) presented a time series model to predict the battery degradation path based on historical paths and partial paths. The proposed model was validated by simulations that were able to work without capacity plunge and were reliable with the inputs of complete historical paths. With the rapid development of battery aging detection and health prediction technologies, the EV battery systems will be safer and more reliable.

Thermal runaway

Battery thermal runaway is a series of extreme exothermic chain reactions which generate excessive heat due to the combustion of battery chemical materials (Arora et al., 2016). Roth et al. (Roth et al., 2004) divided thermal runaway processes into three major phases: the onset phase, accelerated heat generation phase, and the explosion phase. During normal battery operations, heat generation mainly comes from resistive Joule heat and chemical enthalpic heat (Catherino, 2006). With the safe clearances formed by separators, chemistry energy is converting smoothly and safely into useful electricity. If the battery temperature reaches the threshold of thermal runaway, the cavities would have several intensive chemical reactions and produce a large amount of heat and gas. Wang et al. (Wang et al., 2006) and Spotnitz et al. (Spotnitz and Franklin, 2003) discovered that the SEI layer would launch exothermic decomposition processes during 90°C–130°C, producing combustion gases from the reactions between cathodes and electrolytes. At around 135°C, polymer separator materials started to melt, increasing short circuit risk between anodes and cathodes (Wang et al., 2012b). Instantaneous heat and gas abruptions as well as explosive

decompositions are usually observed at around 200°C (Doughty, 2006). The over-accumulated heat could destroy cathodes at over 200°C and burn off flammable gas from electrolytes with the oxygen from the atmosphere. The uncontrolled rupture and explosion would happen if the internal pressures exceeded safety pressures. The vibrant and overheated gases would further damage the separators and generate more extensive heat and gas at 500°C (Zhao et al., 2015). Thermal runaway is a serious safety issue for most battery types, including the ASSB. Although it has solid polymeric or ceramic electrolytes without a separator, which usually could not completely prevent the internal short-circuiting, the oxygen released by the cathode and the anode of the ASSB could still react and cause a serious thermal runaway issue (Liu et al., 2018). For the EV batteries, thermal runaway is usually triggered by improper charging/discharging, short circuit by physical penetration or coolant leakage, or other mechanical abuses such as collisions and accidents, etc. (Xiong et al., 2020).

The first method to prevent thermal runaway is to improve the battery component materials such as separator and electrolyte. Li et al. (Li et al., 2017b) reported a novel flexible and porous separator with high fire resistance, electrolyte wettability, and thermal stability. The crosslinked network structure hybridizing between hydroxyapatite nanowires and cellulose fibers could preserve its structural integrity at 700°C and effectively reduce the risk of thermal runaway. The non-flammable aqueous-based electrolyte Li-ion battery has been showing a significantly low risk of thermal runaway by its extraordinary non-flammable properties, which could be used in the high-safety demand EV applications (Suo et al., 2015; Kim et al., 2014). Gu et al. (Gu et al., 2020) introduced a non-flammable electrolyte made of 25 wt% tris (2,2,2-trifluoroethyl) phosphate and propylene carbonate to improve battery safety and deliver better cycle performance at elevated temperatures (60°C). Moreover, the safety design of the state-of-the-art BTMSs should not only consider heat dissipation but also strengthen the prevention of the thermal runaway propagation (Feng et al., 2020). Feng et al. (Feng et al., 2018a) proposed a three-level protection design to reduce the risk of thermal runaway. The three levels were precautionary warning and passive protection, material intrinsic stability improvement, and secondary thermal runaway shutdown. Zhao et al. (Zhao et al., 2021c) used four fire extinguishing agents to inhibit thermal runaway and its propagation among LIB cells. They found water spray delivered the highest suppressing performance while the Novec 1230 showed the top fireproof characteristics. Lastly, the battery manufacturing defects such as component mechanical deformations, uneven coatings on electrodes, bumpy connections between separators and electrodes, delamination, and contamination of electrolytes, would all cause disastrous consequences. In the last stage of mass production, Toyota Prius improved battery assembly processes to prevent excessive heating risk and thermal runaway incidents (Beauregard and Phoenix, 2008).

Battery thermal management system

The suitable operating temperature is a critical factor to battery output performance, longer service life, and the prevention of thermal runaway. An efficient and robust BTMS is essential to control the maximum operating temperature within an ideal range as well as maintain an even temperature distribution among all the battery cells. Air-cooling and liquid-cooling are two major methods for commercial EV BTMS applications while some other novel cooling technologies such as phase change material (PCM) and heat pipe (HP) methods are very hot research topics in recent years but have not been commercially adopted yet.

The air-cooling approach is mostly used for prismatic battery packs. Chen et al. (Chen et al., 2019a) improved the flow pattern of an air-cooling BTMS for prismatic battery cells by modifying the inlet and outlet of air flow position. Shi et al. (Shi et al., 2021) optimized ten factors of an air-cooling BTMS for LFP prismatic battery pack by an artificial intelligence nine-layer deep learning network model. The optimized system could reduce the temperature difference by 40.36% compared to the original design. Some recent research focused on the application of air-cooling BTMS for the cylindrical cell battery pack. Zhao et al. (Zhao et al., 2021a) proposed a novel gradient vertical spacings design for the cell arrangement to obtain better cooling performance for 21,700 cylindrical cells.

The liquid-cooling method is the mainstream approach for most medium or higher power commercial EV BTMSs with both prismatic and cylindrical cells. Wang et al. (Wang et al., 2017a) design a new type of liquid-cooling BTMS with thermal silica plates for prismatic Li-ion cells. More plate and channel quantities were proven to decrease the maximum temperatures by both experiments and simulations. Karthik et al. (Karthik et al., 2021) used a multi-objective optimization technique to optimize a liquid-cooling BTMS design. The optimal solution set obtained by the multi-objective genetic algorithm method could reduce the maximum

mass flow rate, pressure, and power consumption by 66.33%, 38.10%, and 43.56%, respectively. For the cylindrical cells, Wang et al. (Wang et al., 2020a) designed a novel modular liquid-cooling BTMS to explore the influences of coolant flow rate and cooling mode. The results showed that parallel cooling with increased coolant flow rate was the most effective design to reduce maximum temperature and improve temperature uniformity. Li et al. (Li et al., 2021b) used the Gaussian process model to establish a multi-objective optimization model to optimize the coolant velocity and reduce the pressure drop. The U-shaped channel was proven to be able to significantly reduce the pressure drop loss compared with the serpentine channel.

PCM cooling has the advantages of low parasitic power consumption, uniform temperature distribution character, and low weight (Murali et al., 2021). However, low thermal conductivity, complex structure, and leakage problems are the intrinsic bottlenecks of its further commercial applications. It is usually coupled with other active cooling methods such as air or liquid cooling to enhance thermal conductivity and heat dissipation. Yang et al. (Yang et al., 2021b) designed a novel shark-skin microstructure heat sink as the container of PCMs used in air-cooling based BTMS. The bionic structure was proven to successfully enhance the cooling performance compared with the basic design. Gao et al. (Gao et al., 2021) coupled liquid cooling with PCMs methods for a novel BTMS design. The hybrid structure with double s-shaped microchannels was proven to deliver better heat dissipation than the pure PCM structure.

Similar to PCM structure, HP is also accompanied by other cooling methods as an auxiliary heat dissipation structure due to its efficient heat conduction rate and no parasitic power consumption. Abbas et al. (Abbas et al., 2021) developed a compact BTMS with PCMs, flat plate HPs, and liquid cooling. The HP-attached system could successfully manage the operating temperatures within a required range. Jin et al. (Jin et al., 2021) combined HPs and composite boards into a coupled BTMS. The coupled design was proven to be more effective than the single composite board design. Yao et al. (Yao et al., 2021) proposed an HP and refrigerant-cooling coupled BTMS. Its cooling performance was proven under different ambient temperatures and battery heat generation rates.

Kim et al. (Kim et al., 2019a) recommended that the appropriate BTMS design should combine various cooling methods to compensate for the disadvantages of each other according to the purpose of the EV. An integrated BTMS with refrigerant cooling, PCM, HP, and thermoelectric systems might be suitable for the future advanced EV batteries of high energy density. Akinlabi et al. (Akinlabi and Solyali, 2020) reviewed recent research on the air-cooling BTMS techniques. Parameter configuration optimization and optimization algorithms were classified and identified for improving the air-cooling BTMS designs. Zhao et al. (Zhao et al., 2021b) collated the recent air-cooling BTMS research and found that cooling channel improvement, novel thermally conductive materials, and conjugated cooling systems might be the optimal solutions for future EV and HEV battery packs. Luo et al. (Luo et al., 2021) reviewed recent PCM-based BTMS research and pointed that inorganic material, more thermally conductive structures, better encapsulation, and hybrid systems might be the future research direction for PCM technology. Fayaz et al. (Fayaz et al., 2021) reviewed different optimization algorithms for BTMS design and suggested future research to put more emphasis on the topics such as radiation effect, passive thermal management systems, cylindrical cells, and PCM materials.

THEORETICAL MODELS

Electrical and electrochemical models are the two main battery theoretical models (Nikdel, 2014). The former one reflects battery electrical characteristics and is more comprehensible by using passive linear elements. The latter one precisely involves internal electrochemical actions and is more accurate. Chen et al. (Chen and Rincon-Mora, 2006) proposed an elaborate runtime-based electrical model, considering dynamic parameters such as OCV, current, cycle number, temperature, storage capacity etc. Cun et al. (Cun et al., 1996) used a simplified model of the ideal voltage source and internal resistance to monitor the sealed UPS battery products during a constant power supply. Some researchers used the Thevenin battery model (Daowd et al., 2010; Williamson et al., 2004) which was composed of cell voltage, internal resistance, overvoltage resistance, and capacitor. Because these parameters were supposed to be constant instead of being real-time related to factors such as SOC, capacity, discharging, and temperature, the Thevenin battery model and linear electrical models were not accurate enough. Salameh et al. (Salameh et al., 1992) designed a battery equivalent circuit for a lead-acid battery. The non-linear mathematical model accurately described the battery performance by temperature compensations. Lin et al. (Lin et al., 2000)

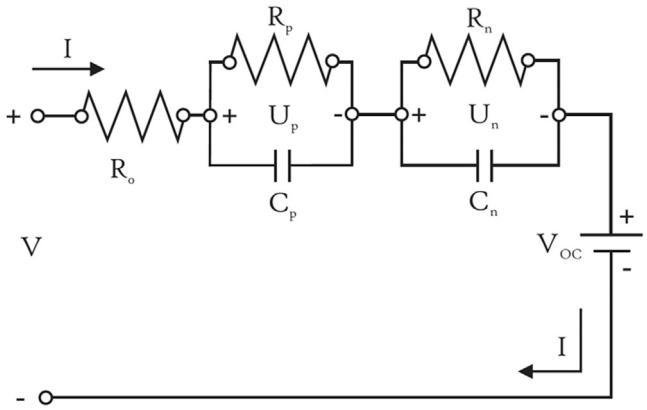

Figure 5. Schematic ECM diagram for LFP battery.

proposed a fractional-order model to simulate dynamic operations. To meet new demands in the automobile industry, simplified fractional-order models were further developed to capture battery dynamics at high-frequency engine cranking operations on EVs (Cugnet et al., 2009; Sabatier et al., 2010).

Zhang et al. (Zhang et al., 2017a) proposed an equivalent circuit model (ECM) in Figure 5 for the LFP battery considering the electrochemical properties to find the relationship between resistances/capacitances and electrochemical parameters in operations of different discharging rates and cycle numbers. Lin et al. (Lin et al., 2012) designed an online identification scheme to monitor parameters based on available onboard signals for cylindrical LFP battery thermal models to estimate their core temperatures. Bernardi et al. (Bernardi et al., 1985) developed a basic energy balance equation to predict battery thermal performance. Chen et al. (Chen and Evans, 1993) designed a 2D model of the multicell system to obtain the basic thermal behavior of lithium/polymer-electrolyte batteries and explored the feasibility of scaling up prototypes with good heat dissipation performance. They found that during high-rate discharging, thinner cell stacks were preferable in terms of less temperature rise and smaller temperature gradients across the battery pack (Chen and Evans, 1994). Giuliano et al. (Giuliano et al., 2011) applied thermochromic liquid crystals to measure the surface temperature field of the Li-Ti battery in the laboratory to observe the thermal performance and cooling efficiency of an active battery cooling system. Zou et al. (Zou et al., 2018) highlighted fractional-order models for the advanced BTMS. These modeling mechanisms had the ability to preserve important parameters to predict system behaviors accurately. Zhang et al. (Zhang and Chow, 2010) developed a series-connected RC parallel circuit model to simulate the battery relaxation effect. The model was a compromise of maximum accuracy and minimal calculation. Tremblay et al. (Tremblay et al., 2007) developed a concise generic battery model using SoC as a state variable to avoid algebraic loop issues. A universal battery parametric model was carried out by Prieto et al. (Prieto et al., 2009) for different types of batteries based on parametric implementations. Different blocks represent different battery behavior based on corresponding battery technologies and appropriate equations. Table 5 generalizes some battery theoretical models and equations. Hu et al. (Hu et al., 2018) established and parameterized a fractional-order calculus ECM (via a Hybrid Genetic Algorithm/Particle Swarm Optimization method) which predicts both SoC and SoH simultaneously by adopting a dual fractional-order extended Kalman filter. The moderately complex state-of-the-art model improved the SoC and SoH estimation error within 1% and its sustainability over the battery aging disturbances was validated by experiments. Deng et al. (Deng et al., 2020a) proposed a regular and autoregressive data-driven Gaussian process regression model to tackle the conundrum of simulating a battery pack of hundreds of inconsistent cells. The autoregressive model was proven to be more accurate in predicting the battery SoC with a lower error and a narrower CI. Deng et al. (Deng et al., 2020b) proposed a feature extraction method to obtain Li-ion battery health indicators from the data of general discharging operations such as acquiring the discharging capacity differences from the discharge voltage curve via a voltage partition strategy and obtaining dynamic discharging voltage curves by a filtering strategy. The Gaussian process regression data-driven method was proven to be the most accurate method among four typical methods to estimate the battery SoH by processing the above health indicators information. For ASSB modeling, Deng et al. (Deng et al., 2020c) applied several model reduction methods to acquire a physics-based reduced-order model using the Laplace transform to derive analytical solutions, using the Padé approximation method to obtain lower-order fractional transfer functions, and using

Table 5. Battery theoretical models and equations

Category	Type	Model	Equation	Relevant parameters	References
Lead-acid battery	–	Third-order model	Equivalent electric circuits	Battery capacity, resistance, capacitance, SoC	Ceraolo, 2000; Barsali and Ceraolo, 2002
	Hawker Genesis 42-Ah rated gelled battery	Dynamic electrical battery model	Non-linear function for maximum available energy	Battery storage capacity, internal resistance, self-discharge resistance, electric losses, temperature dependence	Dürr et al., 2006
Ni-MH battery	–	Thermal-electrochemical coupled model	Thermal energy conservation and lumped-parameter thermal equations	Microscopic diffusion of proton/hydrogen, oxygen reactions, heat transfer coefficient, cell current, OCV, cell voltage	Gu and Wang, 2000
	Three-layer prototype battery pack	Arrhenius equation-based model	Arrhenius equation, least-squares algorithm	Temperature, current rate, depth of discharge	Yang et al., 2013
Li-based battery	Automotive grade battery	Accurate SoC prediction model	Peukert's equation	Current, temperature, SoC	Hausmann and Depcik, 2013
	EV Fleet	A hybrid artificial neural network empirical model with a lumped capacitance EV thermal model	Energy balance equations	Current, battery temperature, SoC, heat capacity, heat transfer coefficient	Lindgren and Lund, 2016
	–	First-order RC model	Recursive least squares (RLS) method, adaptive extended Kalman filter (AEKF), Elman neural network	Internal resistance, polarization resistance, polarization capacitance, loading current, OCV, polarization voltage, terminal voltage	Li et al., 2019b

(*Continued on next page*)

Table 5. *Continued*

Category	Type	Model	Equation	Relevant parameters	References
LFP battery	Single cylindrical battery	Lumped thermal model	Two-state approximation of radially distributed thermal equation	Current, internal resistance, thermal resistance, convection resistance, coolant flow rate	Lin et al., 2012
	Laminated stack plate pouch battery	Lumped 1D electrochemical-2D thermal model	Electrochemical-thermal model governing equations	C-rate, thermal contact resistance, external circuit electrical resistance	Ye et al., 2014
	Cylindrical battery	Combined an equivalent-circuit electrical model and a two-state thermal model	Equivalent circuit equation, two-state thermal equation	SoC, terminal voltage, battery surface temperature, battery core temperature	Lin et al., 2014
	Commercial 18650 battery	Pseudo 2D electrochemical coupled with lumped thermal model	Electrochemical and thermal model equation, Peukert equation	Reaction heat, ohmic heat, reversible heat	Saw et al., 2013
	124 commercial $LiFePO_4$/graphite cells	Feature extraction method, voltage partition strategy, filtering strategy	Linear regression, support vector machine, relevance vector machine, and Gaussian process regression	Health indicators (incremental capacity, differential voltage)	Deng et al., 2020b
$Li_xMn_2O_4$ battery	–	Multi scale multi-dimensional physic-based model	Combined mass transfer, charge balance, electric kinetic, Joule equation, and energy equations	Heat generation rate, voltage, temperature distribution, current distribution	Tourani et al., 2014
	Spiral-wound cylindrical Lithium-ion battery	2D transient mathematical mode	2-way coupling of electrochemical and thermal equations of charge	Discharge rate	Somasundaram et al., 2012
	Battery pack	E-Q diagram graphical model	Thermal-electro-coupled dynamic function	Capacity, Electric quantity	Feng et al., 2018b
$LiNi_xCo_yMn_zO_2$ lithium-ion battery	Multiple cells in parallel	Pseudo 2D first-principle model comprised of different contributions	ANOVA for non-linear models, individual multi-parametric sensitivity analysis	C-rate, electrolyte diffusivity, electronic conductivity, resistance	Vazquez-Arenas et al., 2014
	–	Electrochemical-thermal (ECT) coupling model	Proposed parameter estimation method, excitation response analysis	C-rate, dynamic load current	Li et al., 2016b

(*Continued on next page*)

Table 5. *Continued*

Category	Type	Model	Equation	Relevant parameters	References
$LiCoO_2$ (LCO) battery	–	An impedance-based electric-thermal model coupled to a semi-empirical aging model	Mathematical parametric aging function	Temperature, SoC, impedance, capacity	Ecker et al., 2012
Li-ion NMC battery	Commercial pouch-type Lithium polymer battery	Electrical and thermal model	Energy conservation equation with uniform flow distribution assumption	Cell voltage, cell current, mass, momentum	Chung and Kim, 2019
	Battery pack of NMC battery	Data-driven and feature extraction method	Gaussian process regression, squared exponential kernel function, automatic relevance determination	Dynamic cycles, temperatures, aging conditions	Deng et al., 2020a
	Tiankang™ Battery	Universal mathematical battery model	Charging curve transfer function, genetic algorithm optimization	Charging current, charging rate	Yao et al., 2014
Li-Ti (LTO) battery	Cylindrical 3.03-Ah $LiNiCoAlO_2$ battery	Equivalent Circuit Model (Data-reliant lumped parameter model)	Pulse-multisine signal design methodology, model parameter estimation	SoC, battery temperature, amplitude, bandwidth	Widanage et al., 2016
Li-S battery	–	1D continuum model, Multi-step elementary kinetic model	Evolution of solid phases in the carbon/sulfur composite cathode and multi-components mass and charge transport in the liquid electrolyte, anode Li/Li+ oxidation reaction, cathode six-step polysulfide reduction mechanism	Charge and discharge profiles, electrochemical impedance spectra	Fronczek and Bessler, 2013
	–	Thermodynamically consistent and fully reversible continuum model	Simplified four-step electrochemistry including a simple polysulfide shuttle effect	Discharge curve, current density, Coulombic efficiency	Hofmann et al., 2014
Li-ion ASSB	Li-ion ASSB	Reduced-order model	Partial differential equations, concentration distribution, Pade approximation method	Equilibrium potential, overpotentials, battery voltage	Deng et al., 2020c

(Curry, 2017).

parabolic and cubic functions to approximate concentration distributions successively. The proposed model showed an excellent balance between accuracy and efficiency in comparison to the original physics-based model. To develop the on-board physics-based models for ASSBs, Deng et al. (Deng et al., 2021) analyzed a typical model's parameter sensitivity accurately using different principle methods and constructed a non-linear state-space model to conduct a joint estimation of both the Li-ion concentration states and model parameters using the Sigma point Kalman filter algorithm. The novel physics-based method was validated through three different experiments with small mean absolute errors of the estimated voltages (<2.1 mV) and SoCs (<1.5%).

MANUFACTURING AND COST

As one of the most successful EV batteries, the 18,650 cylindrical Li-ion battery exhibits superiorities of high specific energy, manufacturing automation, and safety performance. On the other hand, more cylindrical cells are needed to provide enough power and capacity for high-performance EVs due to their smaller volume compared with the prismatic and pouch cells. To increase the rated capacity of 18,650 cells, 21,700 cylindrical cells are developed as an upgrade substitution recently. Table 6 compares the specifications of several premium commercial cylindrical Li-ion batteries.

The rated capacity of 21,700 cells is increased by approximately 30%–50% on average. The lithium price is soared by about 65% before 2018 due to agitated market speculations, but the average prices of Li-ion batteries kept dropping from $1100/kWh to $156/kWh. The manufacturing cost of 18,650 cells decreased from around $10 (1,500mAh) to less than $2 (3,000mAh). Because the predicted market size of the Li-ion batteries would be continuously growing in the next decade according to the prediction in Figure 6 (Curry, 2017), their target price would probably drop to less than $100/kWh by 2025.

Although the Li-ion battery technology has been developed rampantly, the Ni-MH battery remains to be an important player in the EV market (Young, 2018). Ni-MH products such as 250-Ah electric bus prismatic cells and 6-Ah HEV multicell battery modules have been produced in commercial scales (Fetcenko et al., 2007). Toyota decided to keep the Ni-MH battery pack for its 2015 model (Fileru, 2015). On the other hand, Fitch forecasted that the market share of NMC batteries would skyrocket to about 63% by 2027. The main uncertainty of its future is the highly unstable cobalt prices due to potential political unrest of the Democratic Republic of the Congo, which is a major cobalt-producing country. Some researchers focus on developing cobalt-free cathodes for LIBs to relieve the increasing reliance on cobalt (Gourley et al., 2020). High cost-performance LFP batteries will be more favored by BYD and NIO to be a major player in the Chinese EV battery market. Tesla keeps improving its NCA cylindrical batteries with sophisticated BMS for its hot-sale models. Table 7 lists the specifications of some mainstream onboard batteries on hot-sale EVs. The onboard power battery selection is a sophisticated and comprehensive balance between capacity, quality, safety, and cost. It is impossible to conclude which battery is the best. OEMs have their strategic planning of the power battery technical route to find the perfect match which is most suitable and compatible with their EV products.

For the manufacturing process optimization, Liu et al. (Liu et al., 2021b) underscored the drying and coating processes research and stressed the importance of the potential industrialization of dry coating technology. Duffner et al. (Duffner et al., 2021) developed a comprehensive cost model to improve the cost efficiency of cell manufacturing for the large-scale cell plant based on the analysis of over 250 parameters by the process-based cost modeling technique. The novel model could provide the direction to the minimum costs as well as the most influential cost elements for cost reductions. Turetskyy et al. (Turetskyy et al., 2020) presented a data-driven concept to identify and evaluate the interdependencies between technical data on the production line and their effects on the cell qualities and properties. Liu et al. (Liu et al., 2021b) reviewed the current major battery manufacturing steps including calendaring, heat drying, slurry casting, and planetary mixing. They suggested that advanced manufacturing technologies such as robotics, laser slitting, dry printing, and ultrasonic mixing could be adopted to increase efficiency and reduce overall cost. Kübler et al. (Kübler et al., 2017) proposed a cloud-based and simulation-assisted method to improve the battery manufacturing accuracy by a run-to-run control overall battery production line stations. Wood et al. (Wood et al., 2019) identified the SEI and cathode-electrolyte interface (CEI) formation processes, the formation protocols effect, as well as the electrode pores inhibitions by the electrolyte as the three challenges in the Li-ion battery manufacturing processes. Asif et al. (Asif and Singh, 2017) adopted practices of rapid thermal processing, advanced process control, as well as industrial internet of things to minimize

Table 6. The specifications of several premium commercial cylindrical Lithium-ion batteries

Manufacturer	Model	Rated capacity (mAh)	Nominal voltage (V)	Weight (g)	Temperature (°C) charge discharge storage	Energy density (Wh/kg)	Height (mm)	Cell diameter (mm)	Anode diameter (mm)
Panasonic	NCR 18650BF	3,200	3.6	46.5	10 to 45 −20 to 60 −20 to 50	248	65.10	18.24	6.6
SONY	US18650VTC6	3,000	3.6	46.5	–	232	65.2	18.5	7.4
Samsung	INR18650-30Q	3,040	3.61	45.6	–	241	64.85	18.33	–
Great Power	ICR18650	2,600	3.7	–	–	–	65.2	18.5	–
LG Chem	18,650 HE4	2,500	3.6	47.0	0 to 50 −20 to 75 −20 to 60	192	65.2	18.5	–
Sanyo-Panasonic	NCR20700B	4,000	3.6	63	10 to 45 −20 to 60 −20 to 50	224	70.3	20.35	10.5
LISHEN	LR2170SA	4,000	3.65	70	0 to 45 −20 to 60 −20 to 60	206	71.1	21.9	–
Samsung	INR21700-50E	4,753	3.6	69	0 to 45 −20 to 60 −20 to 60	248	70.8	20.25	–
Great Power	21,700	4,700	3.7	–	10 to 45 −20 to 60 −20 to 25	–	71	22	–
LG Chem	INR21700 M50	4,850	3.63	69	0 to 45 −20 to 60 −20 to 60	264	70.15	21.1	–

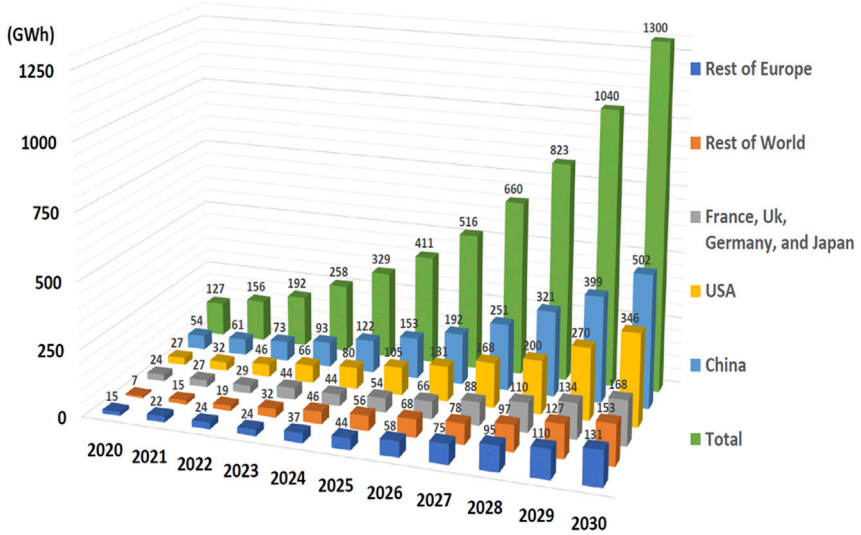

Figure 6. Predicted demands of Lithium-ion batteries for EVs

the cell-to-cell process variations during the battery manufacturing processes. Liu et al. (Liu et al., 2021a) proposed a feature quantification and electrode classification framework based on the random forest method by analyzing four manufacturing features and parameters from the mixing and coating processes. The novel method effectively reduced model dimension and improved the sensitivity analysis of battery manufacturing. Guan et al. (Guan et al., 2021) proposed a refined dehumidification system as the substitution of the conventional desiccant wheel deep-dehumidification system to obtain a coefficient of performance increase from 0.66 to 0.78 based on the on-site performance measurements, effectively reducing the cost of dehumidification. The continuous cost reductions and technology improvements are the main reasons that EVs are becoming more and more competitive over ICE vehicles. Other than manufacturing improvement, Neubauer et al. (Neubauer et al., 2012) stated that driving patterns and charging strategies could all influence the overall lifetime cost of on-board battery packages.

Finally, a good EOL recycling mechanism could also increase the cost efficiency of the battery products (Zeng et al., 2015). LIB recycling is considered as the ultimate approach to handle the EOL EV batteries to leverage fluctuating battery costs, uneven production, and logistic transportation costs (Chen et al., 2019c). Sort and separation technologies, pyrometallurgical and hydrometallurgical processes, as well as direct recycling methods, are all the future research directions and challenges for the commercial EV battery recycling industry. As a mature technology in the mining industry, bioleaching is potentially practical for the metal reclamation in the EOL batteries complementary to the pyrometallurgical and hydrometallurgical processes, especially for the separation of cobalt and nickel which usually require extra solvent-extraction steps to separate (Harper et al., 2019). The microorganisms could digest metal oxides from the collected EOL cathodes and produce metal nanoparticles by reducing cathode oxides. Lander et al. (Lander et al., 2021) comprehensively proposed a techno-economic cost model for EV battery recycling. They found that the transportation, disassembly, scale, and raw material cost are the critical factors for recycling profits. The deep collaborations between academia and industry are strongly recommended to know the real demands of recycling technologies and material testing standards (Ma et al., 2021). The scaling up is beneficial to the economic success of the recycling business in terms of bringing more profits and closing the huge gap between manufacturing and recycling.

DISCUSSION

The battery industry is a comprehensive field of material science, chemistry, electrochemistry, physics, and thermodynamics. Multi-disciplinary skills and efforts are required for its future development. Studies and experiments about battery chemical compositions, morphology structures, and chemical/electrochemical/thermal performances are the methodologies to explore better electrode, electrolyte, and separator materials to make better onboard power batteries. On the other hand, as the EV industry keeps growing,

Table 7. Specifications of some power batteries on hot-sale EVs

Batterytype	Battery manufacturers	EV Model	Capacity (kWh)	Nominal driving range (km)	References
NA	Panasonic	Tesla Model S 75D	75	405	Zubi et al., 2018
		Tesla Model S 90D	90	445	
		Tesla Model S 100D	102	510	
		Tesla Model S P100D	102	505	
LCO	Panasonic, CATL	Tesla Roadster (2020)	200	1,000	Hussein and Massoud, 2019
		Daimler Benz Smart Fortwo Electric Drive	18	120	Zubi et al., 2018
LFP	BYD, GS Yuasa, Lishem, Valence	BYD E6	82	390	Zubi et al., 2018
		Mitsubishi iMiEV	16	95	
NMC	CATL, Hitachi, LG Chem, Samsung SDI, Panasonic, SK Innovation	Chevrolet Bolt EV	60	350	Zubi et al., 2018
		Chevrolet Volt	18.4	85	Zubi et al., 2018
		Ford Focus Electric	33.5	180	Zubi et al., 2018
		BYD E6	82	390	Zubi et al., 2018
		Roewe Ei5	52.5	301	Deng and Tian, 2020
		Renault Zoe ZE50 R135	41	230	Zubi et al., 2018
		Nissan LEAF	30	170	Zubi et al., 2018
		NIO ES6	70	415	Yue, 2020
		BMW i3	33	180	Zubi et al., 2018
		Hyundai Kona Electric	64	415	Ulrich, 2019
		Audi e-tron 55 Sportback	95	446	Burkert et al., 2021
		Volkswagen e-Golf	35.8	195	Zubi et al., 2018

battery technology will continue to thrive to keep the pace of this promising transportation electrification revolution. McKinsey & Co. anticipated that about 70% of automobile sales in Europe in 2040 would be electric vehicles, indicating an astronomical annual demand, 1,200 GW-hours, which requires an approximately $150 billion investment. The potential profits of the business are so large that neither incumbents nor new entrants would ignore this lucrative niche market. However, another world-renowned consulting company, Boston Consulting Group, dampened the enthusiasm by saying "the stakes are very high", insinuating the potential fierce competition in the future EV power battery market.

As a traditional high cost-performance and commercially viable anode material, graphite delivers reliable capacity and excellent cycling stability (Moradi and Botte, 2016), but its theoretical specific energy is lower than those of other novel anodes such as lithium-metal anodes and Si-based anodes (Zou et al., 2021). Si-based anodes exhibit excellent specific capacity and cycling performances with low costs, but their salient breathing effect and capacity degradation problems limit their commercial applications (Li et al., 2017c). LFP is generally regarded as an excellent cathode material due to its durability, long cycle life, high thermal stability and safety, and low manufacturing cost, but it is still not favored by some OEMs who are seeking higher specific energy and lower self-discharge rate products. High energy density does not necessarily mean high risks. Any negligence or overlook of the existing safety standards during the R&D and manufacturing processes could lead to the production of the unqualified battery cells. The defective rate might be extremely low, but the risk of disastrous results will be exponentially amplified by the large-scale productions. Owing to the most critical safety concerns, the battery cells with solid electrolytes and inflammable materials will be more popular in the future high energy commercial battery packages for the OEMs.

Undoubtedly, the outstanding qualities of high energy density, low self-discharge rate, almost no memory effect, high OCV, as well as long cycle life will continuously help Li-ion batteries dominate the EV energy storage device market over most of the contenders (Kim et al., 2019b). Their reliability and feasibility for the deployment in EVs had drawn and would still be drawing exclusive attention from the global OEMs to replace their conventional ICE products in the next decade (Cano et al., 2018; Li et al., 2014). With the gradual but continuous increase of specific

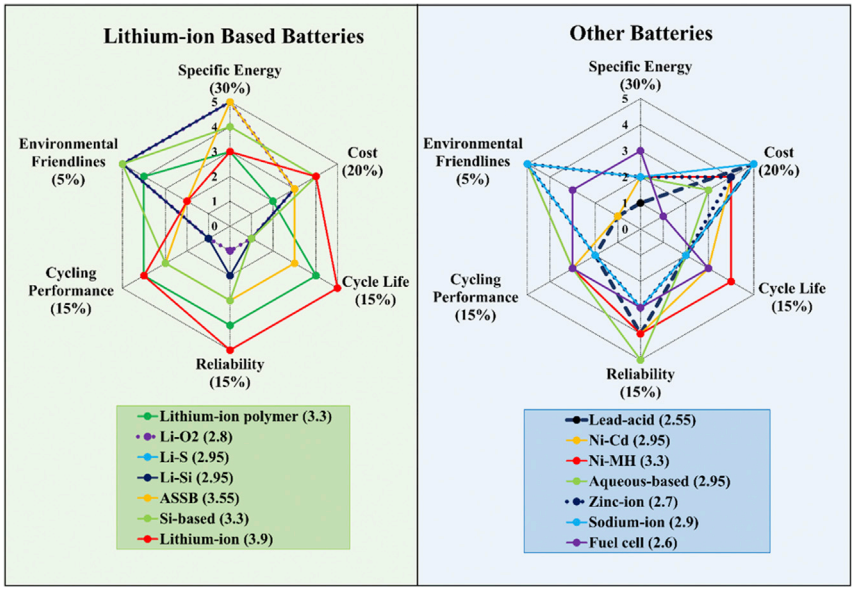

Figure 7. Evaluations of most reigning or potential EV battery technologies with six aspects

power and energy, it is foreseeable that the LFP cell will be more favorable for commercial EV applications due to its supreme safety in a short term. Yang et al. (Yang et al., 2021c) developed a thermally modulated LFP cell which was capable of delivering a sufficient cruise range by just a 10 min fast charging in all climates, effectively alleviating drivers' range anxiety. Ni-MH battery is another but less commonly used onboard power battery due to its relatively high specific power, long cycle life, superb reliability, and outstanding cost performance (Young et al., 2013; Qiao et al., 2019). Fuel cell such as hydrogen-oxygen fuel cell is becoming an efficient and clean energy storage device at some level, but their overall cost is still much higher than the Li-ion battery (Stambouli, 2011). Some state-of-the-art rechargeable batteries, such as Si-based anode battery, ASSB, Li-S battery, and metal-air battery are still not thermally stable, technically reliable, and commercially rewardable, but they all have the potentials to be commercially successful inventions and symbolize the revolutionary future of the next-generation rechargeable battery technologies. From a long-term perspective, the ASSB cell will be a competitive candidate for the onboard EV energy storage systems as a perfect combination of high specific energy and safety if its technical bottlenecks such as low ionic conductivity and poor interface compatibility are successfully overcome.

Figure 7 comprehensively collated and evaluated the potentiality and feasibility of most reigning and potential battery technologies with six technical and economic aspects to be the next-generation EV power battery. The reasonable trade-off between performance, safety, and the cost is always the priority in battery research and development. In terms of the costs, except for the spot prices of the transition metals, battery second life use is also considered as a solution to reduce the EV overall costs (Martinez-Laserna et al., 2018). For ordinary consumers, the battery cost performance will probably be considered as a key factor for choosing an EV product from numerous models from the shelf. The Li-ion based batteries tower above the other batteries in most aspects at the current stage. Except for the Li-ion batteries (3.9 points) and lithium polymer batteries (3.3 points), the ASSB (3.55 points) and Si-based (3.3 points) batteries show the highest potentials to be the next-generation EV power battery with high specific capacity and safety performance. If their technical maturity could be improved to the level of commercial mass production volumes in the next few years, they will be leading the revolutions of the future EV battery market.

Uncertainty is one of the enchantments of science and technology. The battery evolution is not a Schrodinger's Cat but just a matter of "when and how". There will probably be not one monopoly player but many participants in the future EV energy storage device market. But one thing is for sure, no matter what the next-generation technological breakthroughs will be, the unprecedented cooperation between industrial giants and academic communities will unswervingly create safer, stronger, and cheaper rechargeable onboard energy storage systems to let people embrace a brilliant new world of zero emission and green revolution with higher energy utilization efficiencies, less fossil fuel consumption, and less CO_2 emissions.

CONCLUSIONS

In this research, both the conventional and future battery technologies for EVs were comprehensively reviewed, covering most key aspects such as major component materials, operating characteristics, theoretical models, manufacturing processes, cost analysis, etc. Moreover, this article specially focused on some critical issues in the battery commercial applications and lifecycle management. Topics like accurate health diagnosis, RUL prediction techniques, advanced BTMS designs, and thermal runaway preventions could all further extend battery cycle life and reduce the EV lifecycle costs. Two novel hexagon radar charts were created to make a concise yet all-round evaluation of most reigning and potential EV battery technologies. Some specific conclusions were drawn:

1) In a short-term, Li-ion batteries, such as NCM, LMO, LFP etc., would be continuously dominating the onboard power battery market due to their superb properties including high specific power, no memory effect, low self-discharge, as well as long cycle life.
2) In a foreseeable future, some cutting-edge battery technologies such as ASSB, Si-based anode battery, and Li-S battery are ready to be the next-generation commercial EV batteries once they are more thermally stable, technically reliable, and economically rewardable.
3) Battery aging detection and health prediction technologies could effectively enhance the safety and reliability of EV battery systems. The RUL prediction will be more accurate and efficient with the help of advanced numerical models and monitoring methods.
4) The battery thermal energy management system plays an important role in securing battery performance, ensuring service life, and preventing thermal runaway.
5) The manufacturing costs of the batteries could be further reduced by advanced processes control methods and various numerical auxiliary improvement approaches including artificial intelligence analysis and data-driven optimization. But there will be a ceiling for the battery cost reduction due to limited yields and fluctuating spot prices of some critical materials including lithium, cobalt, nickel, etc.
6) Other than the endless pursuit of the higher battery specific power and energy, the Zn-ion and Na-ion batteries might be the promising cheaper and safer substitutions of Li-ion batteries with a reasonable trade-off between capacity and cost due to their ample crust storage while the spot price of lithium has been rocketing with the increasing demand of the Li-ion batteries.

ACKNOWLEDGMENTS

The authors gratefully acknowledge the financial support provided by the Australian Research Council (LP170100879).

AUTHOR CONTRIBUTIONS

Conceptualization: G.Z., X.W., and M.N. Writing of Original Draft: G.Z. Revision: G.Z., X.W., and M.N. Supervision: X.W. and M.N. Funding Acquisition: X.W. and M.N.

DECLARATION OF INTERESTS

The author declares no competing interests. The author does not have any commercial or associative interest that represents a conflict of interest in connection with the work submitted.

REFERENCES

Abbas, S., Ramadan, Z., and Park, C.W. (2021). Thermal performance analysis of compact-type simulative battery module with paraffin as phase-change material and flat plate heat pipe. Int. J. Heat Mass Transfer. *173*, 121269.

Abraham, K., Pasquariello, D., and Schwartz, D. (1989). Practical rechargeable lithium batteries. J. Power Sources *26*, 247–255.

Adams, R.A., Li, B., Kazmi, J., Adams, T.E., Tomar, V., and Pol, V.G. (2018). Dynamic impact of LiCoO2 electrodes for Li-ion battery aging evaluation. Electrochim. Acta *292*, 586–593.

Aifantis, K.E., Hackney, S.A., and Kumar, R.V. (2010). High Energy Density Lithium Batteries: Materials, Engineering, Applications (John Wiley & Sons).

Akinlabi, A.H., and Solyali, D. (2020). Configuration, design, and optimization of air-cooled battery thermal management system for electric vehicles: a review. Renew. Sustain.Energy Rev. *125*, 109815.

Al Hallaj, S., Venkatachalapathy, R., Prakash, J., and Selman, J. (2000). Entropy changes due to structural transformation in the graphite anode and phase change of the LiCoO2 cathode. J. Electrochem. Soc. *147*, 2432.

Alkorta, I., Hernández-Allica, J., Becerril, J., Amezaga, I., Albizu, I., and Garbisu, C. (2004). Recent findings on the phytoremediation of soils

contaminated with environmentally toxic heavy metals and metalloids such as zinc, cadmium, lead, and arsenic. Rev. Environ. Sci. Biotechnol. *3*, 71–90.

Allam, A., Catenaro, E., and Onori, S. (2020). Pushing the envelope in battery estimation algorithms. Iscience *23*, 101847.

Amine, K., Liu, J., and Belharouak, I. (2005). High-temperature storage and cycling of C-LiFePO4/graphite Li-ion cells. Electrochem.Commun. *7*, 669–673. https://doi.org/10.1016/j.elecom.2005.04.018.

Andersen, P.H., Mathews, J.A., and Rask, M. (2009). Integrating private transport into renewable energy policy: the strategy of creating intelligent recharging grids for electric vehicles. Energy Policy *37*, 2481–2486.

Aneke, M., and Wang, M. (2016). Energy storage technologies and real life applications–a state of the art review. Appl. Energy *179*, 350–377.

Anseán, D., Dubarry, M., Devie, A., Liaw, B., García, V., Viera, J., and González, M. (2016). Fast charging technique for high power LiFePO4 batteries: a mechanistic analysis of aging. J. Power Sources *321*, 201–209.

Arora, S., Shen, W., and Kapoor, A. (2016). Review of mechanical design and strategic placement technique of a robust battery pack for electric vehicles. Renew. Sustain.Energy Rev. *60*, 1319–1331.

Asif, A.A., and Singh, R. (2017). Further cost reduction of battery manufacturing. Batteries *3*, 17.

Ates, T., Keller, M., Kulisch, J., Adermann, T., and Passerini, S. (2019). Development of an all-solid-state lithium battery by slurry-coating procedures using a sulfidic electrolyte. Energy Storage Mater. *17*, 204–210.

Baade, P., and Wood, V. (2021). Ultra-high throughput manufacturing method for composite solid-state electrolytes. Iscience *24*, 102055.

Barai, A., Uddin, K., Chevalier, J., Chouchelamane, G.H., Mcgordon, A., Low, J., and Jennings, P. (2017). Transportation safety of lithium iron phosphate batteries-a feasibility study of storing at very low states of charge. Sci. Rep. *7*, 1–10.

Barré, A., Deguilhem, B., Grolleau, S., Gérard, M., Suard, F., and Riu, D. (2013). A review on lithium-ion battery ageing mechanisms and estimations for automotive applications. J. Power Sources *241*, 680–689.

Barsali, S., and Ceraolo, M. (2002). Dynamical models of lead-acid batteries: implementation issues. IEEE Trans. Energ. Convers. *17*, 16–23.

Beauregard, G.P., and Phoenix, A. (2008). Report of Investigation: Hybrids Plus Plug in Hybrid Electric Vehicle (Idaho Falls, ID: US Department of Energy, Idaho National Laboratory).

Bergveld, H.J., Kruijt, W.S., and Notten, P.H. (2002). Battery Management Systems. (Springer).

Bernardi, D., Pawlikowski, E., and Newman, J. (1985). A general energy balance for battery systems. J. Electrochem. Soc. *132*, 5–12.

Berndt, D. (1997). Maintenance-Free Batteries: Lead-Acid, Nickel/Cadmium, Nickel/Hydride (Research Studies Press).

Bertilsson, S., Larsson, F., Furlani, M., Albinsson, I., and Mellander, B.-E. (2017). Lithium-ion battery electrolyte emissions analyzed by coupled thermogravimetric/Fourier-transform infrared spectroscopy. J. Power Sources *365*, 446–455.

Bhangu, B.S., Bentley, P., Stone, D.A., and Bingham, C.M. (2005). Nonlinear observers for predicting state-of-charge and state-of-health of lead-acid batteries for hybrid-electric vehicles. IEEE Trans. Veh. Technol. *54*, 783–794.

Bindra, A. (2020). Electric vehicle batteries eye solid-state technology: prototypes promise lower cost, faster charging, and greater safety. IEEE Power Electron. Mag. *7*, 16–19.

Black, R., Adams, B., and Nazar, L. (2012). Non-aqueous and hybrid Li-O2 batteries. Adv. EnergyMater. *2*, 801–815.

Bodenes, L., Dedryvère, R., Martinez, H., Fischer, F., Tessier, C., and Pérès, J.-P. (2012). Lithium-ion batteries working at 85 C: aging phenomena and electrode/electrolyte interfaces studied by XPS. J. Electrochem. Soc. *159*, A1739.

Bögel, W., Büchel, J.P., and Katz, H. (1998). Real-life EV battery cycling on the test bench. J. Power Sources *72*, 37–42.

Broussely, M., Biensan, P., Bonhomme, F., Blanchard, P., Herreyre, S., Nechev, K., and Staniewicz, R. (2005). Main aging mechanisms in Li ion batteries. J. Power Sources *146*, 90–96.

Bukhari, S.M.a.S., Maqsood, J., Baig, M.Q., Ashraf, S., and Khan, T.A. (2015). Comparison of characteristics–lead acid, nickel based, lead crystal and lithium based batteries. In 2015 17th UKSim-AMSS International Conference on Modelling and Simulation (UKSim) (IEEE), pp. 444–450.

Bullock, K.R., and Laird, E.C. (1982). Self-discharge in acid-starved lead-acid batteries. J. Electrochem. Soc. *129*, 1393.

Burke, A.F. (2007). Batteries and ultracapacitors for electric, hybrid, and fuel cell vehicles. Proc. IEEE *95*, 806–820.

Burkert, A., Fechtner, H., and Schmuelling, B. (2021). Interdisciplinary analysis of social acceptance regarding electric vehicles with a focus on charging infrastructure and driving range in Germany. World Electric Vehicle J. *12*, 25.

Burow, D., Sergeeva, K., Calles, S., Schorb, K., Boerger, A., Roth, C., and Heitjans, P. (2016). Inhomogeneous degradation of graphite anodes in automotive lithium ion batteries under low-temperature pulse cycling conditions. J. Power Sources *307*, 806–814.

Cano, Z.P., Banham, D., Ye, S., Hintennach, A., Lu, J., Fowler, M., and Chen, Z. (2018). Batteries and fuel cells for emerging electric vehicle markets. Nat. Energy *3*, 279–289.

Catherino, H.A. (2006). Complexity in battery systems: thermal runaway in VRLA batteries. J. Power Sources *158*, 977–986.

Ceraolo, M. (2000). New dynamical models of lead-acid batteries. IEEE Trans. Power Syst. *15*, 1184–1190.

Ceylan, M., Sarıkurt, T., and Balıkçı, A. (2014). A novel lithium-ion-polymer battery model for hybrid/electric vehicles. In 2014 IEEE 23rd International Symposium on Industrial Electronics (ISIE) (IEEE), pp. 366–369.

Chatzivasileiadi, A., Ampatzi, E., and Knight, I. (2013). Characteristics of electrical energy storage technologies and their applications in buildings. Renew. Sustain. Energy Rev. *25*, 814–830.

Chen, B., Wang, D., Zhang, B., Zhong, X., Liu, Y., Sheng, J., Zhang, Q., Zou, X., Zhou, G., and Cheng, H.-M. (2021a). Engineering the active sites of graphene catalyst: from CO2 activation to activate Li-CO2 batteries. ACS Nano *15*, 9841–9850. https://doi.org/10.1021/acsnano.1c00756.

Chen, C., Jiang, M., Zhou, T., Raijmakers, L., Vezhlev, E., Wu, B., Schülli, T.U., Danilov, D.L., Wei, Y., and Eichel, R.A. (2021b). Interface aspects in all-solid-state Li-based batteries reviewed. Adv. EnergyMater. *11*, 2003939.

Chen, H., Adekoya, D., Hencz, L., Ma, J., Chen, S., Yan, C., Zhao, H., Cui, G., and Zhang, S. (2020). Stable seamless interfaces and rapid ionic conductivity of Ca–CeO2/LiTFSI/PEO composite electrolyte for high-rate and high-voltage all-solid-state battery. Adv. EnergyMater. *10*, 2000049.

Chen, K., Wu, W., Yuan, F., Chen, L., and Wang, S. (2019a). Cooling efficiency improvement of air-cooled battery thermal management system through designing the flow pattern. Energy *167*, 781–790.

Chen, L., Fan, X., Ji, X., Chen, J., Hou, S., and Wang, C. (2019b). High-energy Li metal battery with lithiated host. Joule *3*, 732–744.

Chen, M., Ma, X., Chen, B., Arsenault, R., Karlson, P., Simon, N., and Wang, Y. (2019c). Recycling end-of-life electric vehicle lithium-ion batteries. Joule *3*, 2622–2646.

Chen, M., and Rincon-Mora, G.A. (2006). Accurate electrical battery model capable of predicting runtime and IV performance. IEEE Trans. Energ. Convers. *21*, 504–511. https://doi.org/10.1109/TEC.2006.874229.

Chen, X., Lei, H., Xiong, R., Shen, W., and Yang, R. (2019d). A novel approach to reconstruct open circuit voltage for state of charge estimation of lithium ion batteries in electric vehicles. Appl. Energy *255*, 113758.

Chen, X., Shen, W., Vo, T.T., Cao, Z., and Kapoor, A. (2012). An overview of lithium-ion batteries for electric vehicles. In 2012 10th International Power & Energy Conference (IPEC) (IEEE), pp. 230–235.

Chen, Y., and Evans, J.W. (1993). Heat transfer phenomena in lithium/polymer-electrolyte batteries for electric vehicle application. J. Electrochem. Soc. *140*, 1833–1838.

Chen, Y., and Evans, J.W. (1994). Thermal analysis of lithium polymer electrolyte batteries by a two

dimensional model—thermal behaviour and design optimization. Electrochim. Acta *39*, 517–526.

Chen, Y., Kang, Y., Zhao, Y., Wang, L., Liu, J., Li, Y., Liang, Z., He, X., Li, X., and Tavajohi, N. (2021c). A review of lithium-ion battery safety concerns: the issues, strategies, and testing standards. J. Energy Chem. *59*, 83–99.

Chen, Y.M., Yu, X.Y., Li, Z., Paik, U., and Lou, X.W.D. (2016). Hierarchical MoS2 tubular structures internally wired by carbon nanotubes as a highly stable anode material for lithium-ion batteries. Sci. Adv. *2*, e1600021.

Chiang, Y.-H., Sean, W.-Y., and Ke, J.-C. (2011). Online estimation of internal resistance and open-circuit voltage of lithium-ion batteries in electric vehicles. J. Power Sources *196*, 3921–3932.

Chiasson, J., and Vairamohan, B. (2003). Estimating the state of charge of a battery. In Proceedings of the 2003 American Control Conference (IEEE), pp. 2863–2868.

Chung, Y., and Kim, M.S. (2019). Thermal analysis and pack level design of battery thermal management system with liquid cooling for electric vehicles. Energy Convers.Manag. *196*, 105–116. https://doi.org/10.1016/j.enconman.2019.05.083.

Conte, F. (2006). Battery and battery management for hybrid electric vehicles: a review. El Elektrotechnik Inf. *123*, 424–431.

Cugnet, M., Sabatier, J., Laruelle, S., Grugeon, S., Sahut, B., Oustaloup, A., and Tarascon, J.-M. (2009). On lead-acid-battery resistance and cranking-capability estimation. IEEE Trans. Ind. Electron. *57*, 909–917.

Cui, M., Wang, L., Guo, X., Wang, E., Yang, Y., Wu, T., He, D., Liu, S., and Yu, H. (2019). Designing of hierarchical mesoporous/macroporous silicon-based composite anode material for low-cost high-performance lithium-ion batteries. J. Mater. Chem. A *7*, 3874–3881.

Cun, J.P., Fiorina, J.N., Fraisse, M., and Mabboux, H. (1996). The experience of a UPS company in advanced battery monitoring. In Proceedings of Intelec'96-International Telecommunications Energy Conference (IEEE), pp. 646–653.

Curry, C. (2017). Lithium-ion battery costs and market. Bloomberg New Energy Finance *5*.

Dan, P., Mengeritski, E., Geronov, Y., Aurbach, D., and Weisman, I. (1995). Performances and safety behaviour of rechargeable AA-size Li/LixMnO2 cell. J. Power Sources *54*, 143–145.

Daowd, M., Omar, N., Verbrugge, B., Van Den Bossche, P., and Van Mierlo, J. (2010). Battery models parameter estimation based on MATLAB/Simulink. In Proceedings of the 25th Electric Vehicle Symposium (EVS-25), Shenzhen, China, 2010 (The 25th World Battery, Hybrid and Fuel Cell Electric Vehicle Symposium & Exhibition), https://www.academia.edu/download/43899134/Battery_Models_Parameter_Estimation_base20160319-30004-18movwp.pdf.

Deng, J., Luo, W.B., Chou, S.L., Liu, H.K., and Dou, S.X. (2018). Sodium-ion batteries: from academic research to practical commercialization. Adv. EnergyMater. *8*, 1701428.

Deng, Z., Hu, X., Lin, X., Che, Y., Xu, L., and Guo, W. (2020a). Data-driven state of charge estimation for lithium-ion battery packs based on Gaussian process regression. Energy *205*, 118000.

Deng, Z., Hu, X., Lin, X., Kim, Y., and Li, J. (2021). Sensitivity analysis and joint estimation of parameters and states for all-solid-state batteries. IEEE Trans. Transport.Electrification *7*, 1314–1323.

Deng, Z., Hu, X., Lin, X., Xu, L., Che, Y., and Hu, L. (2020b). General discharge voltage information enabled health evaluation for lithium-ion batteries. IEEEASME Trans.Mechatron. *26*, 1295–1306.

Deng, Z., Hu, X., Lin, X., Xu, L., Li, J., and Guo, W. (2020c). A reduced-order electrochemical model for all-solid-state batteries. IEEE Trans. Transport.Electrification *7*, 464–473.

Deng, Z., and Tian, P. (2020). Are China's subsidies for electric vehicles effective? Manag.Decis. Econ. *41*, 475–489.

Dolotko, O., Senyshyn, A., Mühlbauer, M., Nikolowski, K., and Ehrenberg, H. (2014). Understanding structural changes in NMC Li-ion cells by *in situ* neutron diffraction. J. Power Sources *255*, 197–203.

Doughty, D.H. (2006). Li ion battery abuse tolerance testing-an overview. Sandia National Laboratories Präsentation auf der AQMD *12*, 1–20.

Du, Y. (2017). Research on the prediction of nickel-metal hydride battery capacity based on artificial intelligence algorithm. Chem. Eng. Trans. *59*, 559–564.

Duffner, F., Mauler, L., Wentker, M., Leker, J., and Winter, M. (2021). Large-scale automotive battery cell manufacturing: analyzing strategic and operational effects on manufacturing costs. Int. J. Prod. Econ. *232*, 107982.

Duong, P.L.T., and Raghavan, N. (2018). Heuristic Kalman optimized particle filter for remaining useful life prediction of lithium-ion battery. Microelectron.Reliab. *81*, 232–243.

Dürr, M., Cruden, A., Gair, S., and Mcdonald, J. (2006). Dynamic model of a lead acid battery for use in a domestic fuel cell system. J. Power Sources *161*, 1400–1411.

Dyer, C.K., Moseley, P.T., Ogumi, Z., Rand, D.A., and Scrosati, B. (2009). Encyclopedia of Electrochemical Power Sources (Elsevier Science & Technology).

Ecker, M., Gerschler, J.B., Vogel, J., Käbitz, S., Hust, F., Dechent, P., and Sauer, D.U. (2012). Development of a lifetime prediction model for lithium-ion batteries based on extended accelerated aging test data. J. Power Sources *215*, 248–257.

Eftekhari, A. (2018). On the Theoretical Capacity/Energy of Lithium Batteries and Their Counterparts (ACS Publications).

Ehinon, K., Naille, S., Dedryvère, R., Lippens, P.-E., Jumas, J.-C., and Gonbeau, D. (2008). Ni3Sn4 electrodes for Li-ion batteries: Li– Sn alloying process and electrode/electrolyte interface phenomena. Chem. Mater. *20*, 5388–5398.

Etacheri, V., Marom, R., Elazari, R., Salitra, G., and Aurbach, D. (2011). Challenges in the development of advanced Li-ion batteries: a review. Energy Environ. Sci. *4*, 3243–3262.

Fan, R., Liu, C., He, K., Ho-Sum Cheng, S., Chen, D., Liao, C., Li, R.K., Tang, J., and Lu, Z. (2020). Versatile strategy for realizing flexible room-temperature all-solid-state battery through a synergistic combination of salt affluent PEO and Li6.75La3Zr1. 75Ta0.25O12 nanofibers. ACS Appl. Mater. Inter. *12*, 7222–7231.

Fan, X., Yue, J., Han, F., Chen, J., Deng, T., Zhou, X., Hou, S., and Wang, C. (2018). High-performance all-solid-state Na–S battery enabled by casting–annealing technology. ACS Nano *12*, 3360–3368.

Fayaz, H., Afzal, A., Samee, A.M., Soudagar, M.E.M., Akram, N., Mujtaba, M., Jilte, R., Islam, M.T., Ağbulut, Ü., and Saleel, C.A. (2021). Optimization of thermal and structural design in lithium-ion batteries to obtain energy efficient battery thermal management system (BTMS): a critical review. Arch. Comput. Methods Eng. *29*, 129–194.

Feng, F., and Northwood, D. (2005). Self-discharge characteristics of a metal hydride electrode for Ni-MH rechargeable batteries. Int. J. Hydrogen Energ. *30*, 1367–1370.

Feng, X., Ouyang, M., Liu, X., Lu, L., Xia, Y., and He, X. (2018a). Thermal runaway mechanism of lithium ion battery for electric vehicles: a review. Energy Storage Mater. *10*, 246–267.

Feng, X., Ren, D., He, X., and Ouyang, M. (2020). Mitigating thermal runaway of lithium-ion batteries. Joule *4*, 743–770.

Feng, X., Xu, C., He, X., Wang, L., Zhang, G., and Ouyang, M. (2018b). Mechanisms for the evolution of cell variations within a LiNixCoyMnzO2/graphite lithium-ion battery pack caused by temperature non-uniformity. J. Clean. Prod. *205*, 447–462.

Fetcenko, M., Ovshinsky, S., Reichman, B., Young, K., Fierro, C., Koch, J., Zallen, A., Mays, W., and Ouchi, T. (2007). Recent advances in NiMH battery technology. J. Power Sources *165*, 544–551.

Fileru, I.F. (2015). Toyota prius–a successful pioneering in hybrid vehicle world. In Applied Mechanics and Materials (Trans Tech Publications), pp. 1139–1144.

Fotouhi, A., Auger, D.J., Propp, K., Longo, S., and Wild, M. (2016). A review on electric vehicle battery modelling: from Lithium-ion toward lithium–sulphur. Renew. Sustain. Energy Rev. *56*, 1008–1021. https://doi.org/10.1016/j.rser.2015.12.009.

Fronczek, D.N., and Bessler, W.G. (2013). Insight into lithium–sulfur batteries: elementary kinetic modeling and impedance simulation. J. Power Sources *244*, 183–188.

Fu, M., Ma, X., Zhao, K., Li, X., and Su, D. (2021). High-entropy materials for energy-related applications. Iscience *24*, 102177.

Gabbar, H.A., Othman, A.M., and Abdussami, M.R. (2021). Review of battery management systems (BMS) development and industrial standards. Technologies *9*, 28.

Gao, L., Liu, S., and Dougal, R.A. (2002). Dynamic lithium-ion battery model for system simulation. IEEE Trans. Compon. Packag.Tech. *25*, 495–505.

Gao, P., Wang, Y., Zhang, Q., Chen, Y., Bao, D., Wang, L., Sun, Y., Li, G., and Zhang, M. (2012). Cadmium hydroxide nanowires–new high capacity Ni–Cd battery anode materials without memory effect. J. Mater. Chem. *22*, 13922–13924.

Gao, Z., Deng, F., Yan, D., Zhu, H., An, Z., and Sun, P. (2021). Thermal performance of thermal management system coupling composite phase change material to water cooling with double s-shaped micro-channels for prismatic lithium-ion battery. J. Energy Storage *45*, 103490.

Garche, J., Dyer, C.K., Moseley, P.T., Ogumi, Z., Rand, D.A., and Scrosati, B. (2013). Encyclopedia of Electrochemical Power Sources (Newnes).

Garche, J., Moseley, P., and Karden, E. (2015). Lead–acid batteries for hybrid electric vehicles and battery electric vehicles. In Advances in Battery Technologies for Electric Vehicles (Elsevier), pp. 75–101.

Gell, R. (2013). A Study of Lead Acid Battery Self-Discharge Characteristics (GELCOservices Pty. Ltd. Automotive Industry Consultants).

Genieser, R., Ferrari, S., Loveridge, M., Beattie, S., Beanland, R., Amari, H., West, G., and Bhagat, R. (2018). Lithium ion batteries (NMC/graphite) cycling at 80 C: different electrolytes and related degradation mechanism. J. Power Sources *373*, 172–183.

Giuliano, M.R., Advani, S.G., and Prasad, A.K. (2011). Thermal analysis and management of lithium–titanate batteries. J. Power Sources *196*, 6517–6524.

Gogoana, R. (2012). Internal Resistance Variances in Lithium-Ion Batteries and Implications in Manufacturing (Massachusetts Institute of Technology).

Gong, Y., Zhang, J., Jiang, L., Shi, J.-A., Zhang, Q., Yang, Z., Zou, D., Wang, J., Yu, X., and Xiao, R. (2017). *In situ* atomic-scale observation of electrochemical delithiation induced structure evolution of LiCoO2 cathode in a working all-solid-state battery. J. Am. Chem. Soc. *139*, 4274–4277.

González-Gil, A., Palacin, R., and Batty, P. (2013). Sustainable urban rail systems: strategies and technologies for optimal management of regenerative braking energy. Energy Convers.Manag. *75*, 374–388.

Gonzalez, M., Perez, M.A., Diaz, J., and Ferrero, F. (1996). Ni-Cd and Ni-MH battery optimized fast-charge method for portable telecommunication applications. In Proceedings of Intelec'96-International Telecommunications Energy Conference (IEEE), pp. 522–529.

Goop, J., Nyholm, E., Odenberger, M., and Johnsson, F. (2019). Impact of electricity market feedback on investments in solar photovoltaic and battery systems in Swedish single-family dwellings. Renew. Energy *163*, 1078–1091.

Gourley, S.W.D., Or, T., and Chen, Z. (2020). Breaking free from cobalt reliance in lithium-ion batteries. Iscience *23*, 101505.

Grande, L., Paillard, E., Hassoun, J., Park, J.B., Lee, Y.J., Sun, Y.K., Passerini, S., and Scrosati, B. (2015). The lithium/air battery: still an emerging system or a practical reality? Adv. Mater. *27*, 784–800.

Gu, M., Song, W.-J., Hong, J., Kim, S.Y., Shin, T.J., Kotov, N.A., Park, S., and Kim, B.-S. (2019). Stretchable batteries with gradient multilayer conductors. Sci. Adv. *5*, eaaw1879.

Gu, W., and Wang, C. (2000). Thermal-electrochemical modeling of battery systems. J. Electrochem. Soc. *147*, 2910–2922.

Gu, Y., Fang, S., Zhang, X., Tang, Y., Chen, Y., Yang, L., and Hirano, S.-I. (2020). A non-flammable electrolyte for lithium-ion batteries containing lithium difluoro (oxalato) borate, propylene carbonate and tris (2, 2, 2-trifluoroethyl) phosphate. J. Electrochem. Soc. *167*, 080524.

Guan, B., Zhang, T., and Liu, X. (2021). On-site performance investigation of a desiccant wheel deep-dehumidification system applied in lithium battery manufacturing plant. Energy Build. *232*, 110659.

Guan, P., Li, J., Lu, T., Guan, T., Ma, Z., Peng, Z., Zhu, X., and Zhang, L. (2018). Facile and scalable approach to fabricate granadilla-like porous-structured silicon-based anode for lithium ion batteries. ACS Appl. Mater. Inter. *10*, 34283–34290.

Guyomard, D., and Tarascon, J.-M. (1992). Li metal-free rechargeable LiMn2 O 4/carbon cells: their understanding and optimization. J. Electrochem. Soc. *139*, 937.

Hadjipaschalis, I., Poullikkas, A., and Efthimiou, V. (2009). Overview of current and future energy storage technologies for electric power applications. Renew. Sustain. Energ. Rev. *13*, 1513–1522.

Halimah, P.N., Rahardian, S., and Budiman, B.A. (2019). Battery cells for electric vehicles. Int. J. Sustain.Transport.Technol. *2*, 54–57.

Hall, J., Schoen, A., Allen, P., Liu, P., and Kirby, K. (2006). Resistance growth in lithium ion satellite cells.I. Non destructive data analyses. In Meeting Abstracts (The Electrochemical Society), p. 242.

Hannan, M.A., Lipu, M.H., Hussain, A., and Mohamed, A. (2017). A review of lithium-ion battery state of charge estimation and management system in electric vehicle applications: challenges and recommendations. Renew. Sustain. Energy Rev. *78*, 834–854.

Harper, G., Sommerville, R., Kendrick, E., Driscoll, L., Slater, P., Stolkin, R., Walton, A., Christensen, P., Heidrich, O., and Lambert, S. (2019). Recycling lithium-ion batteries from electric vehicles. Nature *575*, 75–86.

Hausmann, A., and Depcik, C. (2013). Expanding the Peukert equation for battery capacity modeling through inclusion of a temperature dependency. J. Power Sources *235*, 148–158.

He, P., Quan, Y., Xu, X., Yan, M., Yang, W., An, Q., He, L., and Mai, L. (2017). High-performance aqueous zinc–ion battery based on layered H2V3O8 nanowire cathode. Small *13*, 1702551.

Herreyre, S., Huchet, O., Barusseau, S., Perton, F., Bodet, J., and Biensan, P. (2001). New Li-ion electrolytes for low temperature applications. J. Power Sources *97*, 576–580.

Hofmann, A.F., Fronczek, D.N., and Bessler, W.G. (2014). Mechanistic modeling of polysulfide shuttle and capacity loss in lithium–sulfur batteries. J. Power Sources *259*, 300–310.

Hooftman, N., Messagie, M., Van Mierlo, J., and Coosemans, T. (2018). A review of the European passenger car regulations–real driving emissions vs local air quality. Renew. Sustain. Energy Rev. *86*, 1–21.

Hopkins, B.J., Sassin, M.B., Chervin, C.N., Desario, P.A., Parker, J.F., Long, J.W., and Rolison, D.R. (2020). Fabricating architected zinc electrodes with unprecedented volumetric capacity in rechargeable alkaline cells. Energy Storage Mater. *27*, 370–376.

Hosen, M.S., Jaguemont, J., Van Mierlo, J., and Berecibar, M. (2021). Battery lifetime prediction and performance assessment of different modeling approaches. Iscience *24*, 102060.

Hu, L., and Xu, K. (2014). Nonflammable electrolyte enhances battery safety. Proc. Natl. Acad. Sci. *111*, 3205–3206.

Hu, X., Yuan, H., Zou, C., Li, Z., and Zhang, L. (2018). Co-estimation of state of charge and state of health for lithium-ion batteries based on fractional-order calculus. IEEE Trans. Veh.Technol. *67*, 10319–10329.

Hu, X., Zou, C., Zhang, C., and Li, Y. (2017). Technological developments in batteries: a survey of principal roles, types, and management needs. IEEE Power Energy Mag. *15*, 20–31.

Huang, C., Ji, Q., Zhang, H., Wang, Y., Wang, S., Liu, X., Guo, Y., and Zhang, C. (2022). Ru-incorporated Co3O4 nanoparticles from self-sacrificial ZIF-67 template as efficient bifunctional electrocatalysts for rechargeable metal-air battery. J. Colloid Interf. Sci. *606*, 654–665.

Huang, C.K., Sakamoto, J., Wolfenstine, J., and Surampudi, S. (2000). The limits of low-temperature performance of Li-ion cells. J. Electrochem. Soc. *147*, 2893.

Hussain, A., Arif, S.M., and Aslam, M. (2017). Emerging renewable and sustainable energy technologies: state of the art. Renew. Sustain. Energy Rev. *71*, 12–28.

Hussein, N., and Massoud, A. (2019). Electric vehicle fast chargers: futuristic vision, market trends and requirements. In 2019 2nd International Conference on Smart Grid and Renewable Energy (SGRE) (IEEE), pp. 1–6.

Ibrahim, H., Ilinca, A., and Perron, J. (2008). Energy storage systems—characteristics and

comparisons. Renew. Sustain. Energ. Rev. *12*, 1221–1250.

Iraola, U., Aizpuru, I., Gorrotxategi, L., Segade, J.M.C., Larrazabal, A.E., and Gil, I. (2014). Influence of voltage balancing on the temperature distribution of a Li-ion battery module. IEEE Trans. EnergyConvers. *30*, 507–514.

Iwamura, S., Nishihara, H., Ono, Y., Morito, H., Yamane, H., Nara, H., Osaka, T., and Kyotani, T. (2015). Li-rich Li-Si alloy as a lithium-containing negative electrode material towards high energy lithium-ion batteries. Sci. Rep. *5*, 8085.

Jaguemont, J., Boulon, L., Venet, P., Dubé, Y., and Sari, A. (2015). Lithium-ion battery aging experiments at subzero temperatures and model development for capacity fade estimation. IEEE Trans. Veh.Technol. *65*, 4328–4343.

Jeyaseelan, C., Jain, A., Khurana, P., Kumar, D., and Thatai, S. (2020). Ni-Cd batteries. In Rechargeable Batteries: History, Progress, and Applications, R. Boddula, I. Inamuddin, R. Pothu, and A.M. Asiri, eds. (Wiley Online Library), pp. 177–194.

Jin, X., Duan, X., Jiang, W., Wang, Y., Zou, Y., Lei, W., Sun, L., and Ma, Z. (2021). Structural design of a composite board/heat pipe based on the coupled electro-chemical-thermal model in battery thermal management system. Energy *216*, 119234.

Johnson, C., Kim, J., Lefief, C., Li, N., Vaughey, J., and Thackeray, M. (2004). The significance of the Li2MnO3 component in 'composite'xLi2MnO3·(1−x) LiMn0. 5Ni0. 5O2 electrodes. Electrochem.Commun. *6*, 1085–1091.

Jose, C.P., and Meikandasivam, S. (2017). A review on the trends and developments in hybrid electric vehicles. In Innovative Design and Development Practices in Aerospace and Automotive Engineering (Springer), pp. 211–229.

Kang, B., and Ceder, G. (2009). Battery materials for ultrafast charging and discharging. Nature *458*, 190–193.

Karkera, G., Reddy, M.A., and Fichtner, M. (2021). Recent developments and future perspectives of anionic batteries. J. Power Sources *481*, 228877.

Karthik, A., Kalita, P., Garg, A., Gao, L., Chen, S., and Peng, X. (2021). A novel MOGA approach for power saving strategy and optimization of maximum temperature and maximum pressure for liquid cooling type battery thermal management system. Int. J. Green Energy *18*, 80–89.

Kebede, A.A., Coosemans, T., Messagie, M., Jemal, T., Behabtu, H.A., Van Mierlo, J., and Berecibar, M. (2021). Techno-economic analysis of lithium-ion and lead-acid batteries in stationary energy storage application. J. Energy Storage *40*, 102748.

Kim, B.G., Tredeau, F.P., and Salameh, Z.M. (2008). Performance evaluation of lithium polymer batteries for use in electric vehicles. In 2008 IEEE Vehicle Power and Propulsion Conference (IEEE), pp. 1–5.

Kim, H., Hong, J., Park, K.-Y., Kim, H., Kim, S.-W., and Kang, K. (2014). Aqueous rechargeable Li and Na ion batteries. Chem. Rev. *114*, 11788–11827.

Kim, J., Oh, J., and Lee, H. (2019a). Review on battery thermal management system for electric vehicles. Appl. Therm. Eng. *149*, 192–212.

Kim, J.Y., and Lim, D.Y. (2010). Surface-modified membrane as a separator for lithium-ion polymer battery. Energies *3*, 866–885.

Kim, T., Song, W., Son, D.-Y., Ono, L.K., and Qi, Y. (2019b). Lithium-ion batteries: outlook on present, future, and hybridized technologies. J. Mater. Chem. A *7*, 2942–2964.

Kitamura, N., Korechika, Y., Saruwatari, H., Takami, N., and Idemoto, Y. (2011). Effect of supersonic-wave treatment in Zn aqueous solution on property, crystal structure and cycle performance of LiMn1.5Ni0. 5O4 as a cathode material for 5 V class Li ion battery. Solid State Ionics *183*, 54–59.

Kübler, K., Verl, A., Riedel, O., and Oberle, M. (2017). Simulation-assisted run-to-run control for battery manufacturing in a cloud environment. In 2017 24th International Conference on Mechatronics and Machine Vision in Practice (M2VIP) (IEEE), pp. 1–6.

Kuper, C., Hoh, M., Houchin-Miller, G., and Fuhr, J. (2009). Thermal management of hybrid vehicle battery systems. In EVS24 (Materials Science), pp. 1–10, https://www.semanticscholar.org/paper/Thermal-Management-of-Hybrid-Vehicle-Battery-Kuper-Hoh/24d6ba43686a1e9656c38ca5c7a002fe6991a81d.

Lander, L., Cleaver, T., Rajaeifar, M.A., Nguyen-Tien, V., Elliott, R.J., Heidrich, O., Kendrick, E., Edge, J.S., and Offer, G. (2021). Financial viability of electric vehicle lithium-ion battery recycling. Iscience *24*, 102787.

Leblanc, P., Blanchard, P., and Senyarich, S. (1998). Self-discharge of sealed nickel—metal hydride batteries: mechanisms and improvements. J. Electrochem. Soc. *145*, 844.

Lee, H.C., Park, J.O., Kim, M., Kwon, H.J., Kim, J.-H., Choi, K.H., Kim, K., and Im, D. (2019). High-energy-density Li-O2 battery at cell scale with folded cell structure. Joule *3*, 542–556.

Lee, R., and Brown, S. (2021). Evaluating the role of behavior and social class in electric vehicle adoption and charging demands. Iscience *24*, 102914.

Li, F., Wen, L., and Cheng, H.-M. (2021a). Novel Electrochemical Energy Storage Devices: Materials, Architectures, and Future Trends (John Wiley & Sons).

Li, G., Zhang, J., and He, H. (2017a). Battery SOC constraint comparison for predictive energy management of plug-in hybrid electric bus. Appl. Energy *194*, 578–587.

Li, H., Wu, D., Wu, J., Dong, L.Y., Zhu, Y.J., and Hu, X. (2017b). Flexible, high-wettability and fire-resistant separators based on hydroxyapatite nanowires for advanced lithium-ion batteries. Adv. Mater. *29*, 1703548.

Li, J., Lai, Q., Wang, L., Lyu, C., and Wang, H. (2016a). A method for SOC estimation based on simplified mechanistic model for LiFePO4 battery. Energy *114*, 1266–1276.

Li, J., and Passerini, S. (2021). Introduction to the special issue: focus review-new and emerging battery technologies. J. Power Sources *484*, 229333.

Li, J., Wang, L., Lyu, C., Wang, H., and Liu, X. (2016b). New method for parameter estimation of an electrochemical-thermal coupling model for LiCoO2 battery. J. Power Sources *307*, 220–230.

Li, L., Saldivar, A.a.F., Bai, Y., and Li, Y. (2019a). Battery remaining useful life prediction with inheritance particle filtering. Energies *12*, 2784.

Li, M.-Y., Liu, C.-L., Shi, M.-R., and Dong, W.-S. (2011). Nanostructure Sn–Co–C composite lithium ion battery electrode with unique stability and high electrochemical performance. Electrochim. Acta *56*, 3023–3028.

Li, P., Zhang, Z., Xiong, Q., Ding, B., Hou, J., Luo, D., Rong, Y., and Li, S. (2020). State-of-health estimation and remaining useful life prediction for the lithium-ion battery based on a variant long short term memory neural network. J. Power Sources *459*, 228069.

Li, P., Zhao, G., Zheng, X., Xu, X., Yao, C., Sun, W., and Dou, S.X. (2018a). Recent progress on silicon-based anode materials for practical lithium-ion battery applications. Energy Storage Mater. *15*, 422–446.

Li, W., Garg, A., Xiao, M., and Gao, L. (2021b). Optimization for liquid cooling cylindrical battery thermal management system based on Gaussian process model. J. Therm. Sci. Eng. Appl. *13*, 021015.

Li, X., Liang, J., Li, X., Wang, C., Luo, J., Li, R., and Sun, X. (2018b). High-performance all-solid-state Li–Se batteries induced by sulfide electrolytes. Energy Environ. Sci. *11*, 2828–2832.

Li, X., Wang, Z., and Zhang, L. (2019b). Co-estimation of capacity and state-of-charge for lithium-ion batteries in electric vehicles. Energy *174*, 33–44.

Li, Y., Gao, X., Qin, Y., Du, J., Guo, D., Feng, X., Lu, L., Han, X., and Ouyang, M. (2021c). Drive circuitry of an electric vehicle enabling rapid heating of the battery pack at low temperatures. Iscience *24*, 101921.

Li, Y., Song, J., and Yang, J. (2014). A review on structure model and energy system design of lithium-ion battery in renewable energy vehicle. Renew. Sustain. Energy Rev. *37*, 627–633.

Li, Y., Yang, J., and Song, J. (2017c). Design principles and energy system scale analysis technologies of new lithium-ion and aluminum-ion batteries for sustainable energy electric vehicles. Renew. Sustain. Energy Rev. *71*, 645–651.

Li, Y., Yang, J., and Song, J. (2017d). Design structure model and renewable energy technology for rechargeable battery towards greener and more sustainable electric vehicle. Renew. Sustain. Energy Rev. *74*, 19–25.

Li, Y., Yang, J., and Song, J. (2017e). Efficient storage mechanisms and heterogeneous structures for building better next-generation lithium rechargeable batteries. Renew. Sustain. Energy Rev. *79*, 1503–1512.

Liao, L., Cheng, X., Ma, Y., Zuo, P., Fang, W., Yin, G., and Gao, Y. (2013). Fluoroethylene carbonate as electrolyte additive to improve low temperature performance of LiFePO4 electrode. Electrochim. Acta *87*, 466–472.

Liao, L., Zuo, P., Ma, Y., Chen, X., An, Y., Gao, Y., and Yin, G. (2012). Effects of temperature on charge/discharge behaviors of LiFePO4 cathode for Li-ion batteries. Electrochim. Acta *60*, 269–273.

Lim, J.-H., Bang, H., Lee, K.-S., Amine, K., and Sun, Y.-K. (2009). Electrochemical characterization of Li2MnO3–Li [Ni1/3Co1/3Mn1/3] O2–LiNiO2 cathode synthesized via co-precipitation for lithium secondary batteries. J. Power Sources *189*, 571–575.

Lin, C.-P., Cabrera, J., Yang, F., Ling, M.-H., Tsui, K.-L., and Bae, S.-J. (2020). Battery state of health modeling and remaining useful life prediction through time series model. Appl. Energy *275*, 115338.

Lin, H.-P., Chua, D., Salomon, M., Shiao, H., Hendrickson, M., Plichta, E., and Slane, S. (2001). Low-temperature behavior of Li-ion cells. Electrochem. Solid State Lett. *4*, A71.

Lin, J., Poinot, T., Trigeassou, J.-C., and Ouvrard, R. (2000). Parameter estimation of fractional systems: application to the modeling of a lead-acid battery. IFAC Proc. Vol. *33*, 983–988.

Lin, X., Perez, H.E., Mohan, S., Siegel, J.B., Stefanopoulou, A.G., Ding, Y., and Castanier, M.P. (2014). A lumped-parameter electro-thermal model for cylindrical batteries. J. Power Sources *257*, 1–11.

Lin, X., Perez, H.E., Siegel, J.B., Stefanopoulou, A.G., Li, Y., Anderson, R.D., Ding, Y., and Castanier, M.P. (2012). Online parameterization of lumped thermal dynamics in cylindrical lithium ion batteries for core temperature estimation and health monitoring. IEEE Trans. Control Syst. Technol. *21*, 1745–1755.

Lindgren, J., and Lund, P.D. (2016). Effect of extreme temperatures on battery charging and performance of electric vehicles. J. Power Sources *328*, 37–45. https://doi.org/10.1016/j.jpowsour.2016.07.038.

Liu, C., Wang, Y., and Chen, Z. (2019a). Degradation model and cycle life prediction for lithium-ion battery used in hybrid energy storage system. Energy *166*, 796–806.

Liu, K., Hu, X., Zhou, H., Tong, L., Widanalage, D., and Macro, J. (2021a). Feature analyses and modelling of lithium-ion batteries manufacturing based on random forest classification. IEEE ASME Trans. Mechatron *166*, 796–806.

Liu, P., Wang, J., Hicks-Garner, J., Sherman, E., Soukiazian, S., Verbrugge, M., Tataria, H., Musser, J., and Finamore, P. (2010). Aging mechanisms of LiFePO4 batteries deduced by electrochemical and structural analyses. J. Electrochem. Soc. *157*, A499–A507.

Liu, R., Chen, J., Xun, J., Jiao, K., and Du, Q. (2014). Numerical investigation of thermal behaviors in lithium-ion battery stack discharge. Appl. Energ. *132*, 288–297.

Liu, S., Xu, W., Ding, C., Yu, J., Fang, D., Ding, Y., and Hou, H. (2019b). Boosting electrochemical performance of electrospun silicon-based anode materials for lithium-ion battery by surface coating a second layer of carbon. Appl. Surf. Sci. *494*, 94–100.

Liu, X., Ren, D., Hsu, H., Feng, X., Xu, G.-L., Zhuang, M., Gao, H., Lu, L., Han, X., and Chu, Z. (2018). Thermal runaway of lithium-ion batteries without internal short circuit. Joule *2*, 2047–2064.

Liu, Y., Mi, C., Yuan, C., and Zhang, X. (2009). Improvement of electrochemical and thermal stability of LiFePO4 cathode modified by CeO2. J. Electroanal. Chem. *628*, 73–80.

Liu, Y., Pan, H., Gao, M., and Wang, Q. (2011). Advanced hydrogen storage alloys for Ni/MH rechargeable batteries. J. Mater. Chem. *21*, 4743–4755.

Liu, Y., Zhang, R., Wang, J., and Wang, Y. (2021b). Current and future lithium-ion battery manufacturing. Iscience *24*, 102332.

Liu, Z., Yu, Q., Zhao, Y., He, R., Xu, M., Feng, S., Li, S., Zhou, L., and Mai, L. (2019c). Silicon oxides: a promising family of anode materials for lithium-ion batteries. Chem. Soc. Rev. *48*, 285–309.

Low, W.Y., Aziz, M.J.A., and Idris, N.R.N. (2016). Modelling of lithium-titanate battery with ambient temperature effect for charger design. IET Power Electron. *9*, 1204–1212.

Lu, Z., Yu, X., Wei, L., Cao, F., Zhang, L., Meng, X., and Jin, L. (2019). A comprehensive experimental study on temperature-dependent performance of lithium-ion battery. Appl. Therm. Eng. *158*, 113800.

Luntz, A.C., Mccloskey, B.D., Gowda, S., Horn, H., and Viswanathan, V. (2014). Cathode electrochemistry in nonaqueous lithium air batteries. In The Lithium Air Battery: Fundamentals, N. Imanishi, A.C. Luntz, and P. Bruce, eds. (Springer New York), pp. 59–120.

Luo, J., Zou, D., Wang, Y., Wang, S., and Huang, L. (2021). Battery thermal management systems (BTMs) based on phase change material (PCM): a comprehensive review. Chem. Eng. J. *430*, 132741.

Luo, W., Chen, X., Xia, Y., Chen, M., Wang, L., Wang, Q., Li, W., and Yang, J. (2017). Surface and interface engineering of silicon-based anode materials for lithium-ion batteries. Adv. EnergyMater. *7*, 1701083.

Ma, X., Azhari, L., and Wang, Y. (2021). Li-ion battery recycling challenges. Chem *7*, 2843–2847.

Majumder, S., Nieto, S., and Katiyar, R. (2006). Synthesis and electrochemical properties of LiNi0. 80 (Co0. 20− xAlx) O2 (x= 0.0 and 0.05) cathodes for Li ion rechargeable batteries. J. Power Sources *154*, 262–267.

Markevich, E., Baranchugov, V., Salitra, G., Aurbach, D., and Schmidt, M.A. (2008). Behavior of graphite electrodes in solutions based on ionic liquids in *in situ* Raman studies. J. Electrochem. Soc. *155*, A132–A137.

Markovsky, B., Amalraj, F., Gottlieb, H.E., Gofer, Y., Martha, S.K., and Aurbach, D. (2010). On the electrochemical behavior of aluminum electrodes in nonaqueous electrolyte solutions of lithium salts. J. Electrochem. Soc. *157*, A423–A429.

Martha, S.K., Grinblat, J., Haik, O., Zinigrad, E., Drezen, T., Miners, J.H., Exnar, I., Kay, A., Markovsky, B., and Aurbach, D. (2009). LiMn0. 8Fe0. 2PO4: an advanced cathode material for rechargeable lithium batteries. Angew. Chem. Int. Edition *48*, 8559–8563.

Martinez-Laserna, E., Gandiaga, I., Sarasketa-Zabala, E., Badeda, J., Stroe, D.-I., Swierczynski, M., and Goikoetxea, A. (2018). Battery second life: hype, hope or reality? A critical review of the state of the art. Renew. Sustain. Energy Rev. *93*, 701–718.

Mathieu, R., Martin, C., Briat, O., Gyan, P., and Vinassa, J.-M. (2019). Comparative ageing study of CC-CV fast charging for commercial 18650 Li-ion cells: impact of environmental temperature. In 2019 IEEE Vehicle Power and Propulsion Conference (VPPC) (IEEE), pp. 1–5.

Meng, B., Wang, Y., Mao, J., Liu, J., Xu, G., and Dai, J. (2018). Using SoC online correction method based on parameter identification to optimize the operation range of NI-MH battery for electric boat. Energies *11*, 586.

Meng, Y., Li, J.-C., Zhao, S.-Y., Shi, C., Li, X.-Q., Zhang, L., Hou, P.-X., Liu, C., and Cheng, H.-M. (2021). Fluorination-assisted preparation of self-supporting single-atom Fe-N-doped single-wall carbon nanotube film as bifunctional oxygen electrode for rechargeable Zn-Air batteries. Appl. Catal. BEnviron. *294*, 120239.

Miao, Y., Hynan, P., Von Jouanne, A., and Yokochi, A. (2019). Current Li-ion battery technologies in electric vehicles and opportunities for advancements. Energies *12*, 1074.

Millner, A. (2010). Modeling lithium ion battery degradation in electric vehicles. In 2010 IEEE Conference on Innovative Technologies for an Efficient and Reliable Electricity Supply (IEEE), pp. 349–356.

Ming, J., Guo, J., Xia, C., Wang, W., and Alshareef, H.N. (2019). Zinc-ion batteries: materials, mechanisms, and applications. Mater. Sci. Eng. R Rep. *135*, 58–84.

Mohammadi, F. (2018). Design, analysis, and electrification of a solar-powered electric vehicle. J. Solar Energy Res. *3*, 293–299.

Moradi, B., and Botte, G.G. (2016). Recycling of graphite anodes for the next generation of lithium ion batteries. J. Appl. Electrochem. *46*, 123–148.

Moseley, P.T., Rand, D.A., and Monahov, B. (2012). Designing lead–acid batteries to meet energy and power requirements of future automobiles. J. Power Sources *219*, 75–79.

Moustakas, K., Loizidou, M., Rehan, M., and Nizami, A. (2020). A Review of Recent Developments in Renewable and Sustainable Energy Systems: Key Challenges and Future Perspective (Elsevier).

Moy, D., Manivannan, A., and Narayanan, S. (2015). Direct measurement of polysulfide shuttle current: a window into understanding the

performance of lithium-sulfur cells. J. Electrochem. Soc. *162*, A1–A7.

Mukhopadhyay, A., and Sheldon, B.W. (2014). Deformation and stress in electrode materials for Li-ion batteries. Prog.Mater. Sci. *63*, 58–116.

Murali, G., Sravya, G., Jaya, J., and Vamsi, V.N. (2021). A review on hybrid thermal management of battery packs and it's cooling performance by enhanced PCM. Renew. Sustain. Energy Rev. *150*, 111513.

Nagasubramanian, G. (2001). Electrical characteristics of 18650 Li-ion cells at low temperatures. J. Appl. Electrochem. *31*, 99–104.

Nazari, A., Esmaeeli, R., Hashemi, S.R., Aliniagerdroudbari, H., and Farhad, S. (2018). The effect of temperature on lithium-ion battery energy efficiency with graphite/LiFePO4 electrodes at different nominal capacities. In ASME 2018 Power Conference Collocated with the ASME 2018 12th International Conference on Energy Sustainability and the ASME 2018 Nuclear Forum, *Paper No: POWER2018-7375. V002T09A008* (American Society of Mechanical Engineers Digital Collection), p. 7. https://doi.org/10.1115/POWER2018-7375.

Nelson, R.F., and Wisdom, D.M. (1991). Pure lead and the tin effect in deep-cycling lead/acid battery applications. J. Power Sources *33*, 165–185.

Neubauer, J., Brooker, A., and Wood, E. (2012). Sensitivity of battery electric vehicle economics to drive patterns, vehicle range, and charge strategies. J. Power Sources *209*, 269–277.

Nikdel, M. (2014). Various battery models for various simulation studies and applications. Renew. Sustain. Energy Rev. *32*, 477–485.

Nunotani, K., Yoshida, F., Kamiya, Y., Daisho, Y., Abe, K., Kono, M., and Matsuo, H. (2011). Development and performance evaluation of lithium iron phosphate battery with superior rapid charging performance—second report: evaluation of battery capacity loss characteristics. In 2011 IEEE Vehicle Power and Propulsion Conference (IEEE), pp. 1–4.

Opitz, A., Badami, P., Shen, L., Vignarooban, K., and Kannan, A.M. (2017). Can Li-ion batteries be the panacea for automotive applications? Renew. Sustain. Energy Rev. *68*, 685–692.

Ouyang, L., Huang, J., Wang, H., Liu, J., and Zhu, M. (2017). Progress of hydrogen storage alloys for Ni-MH rechargeable power batteries in electric vehicles: a review. Mater. Chem. Phys. *200*, 164–178.

Ovshinsky, S., Fetcenko, M., and Ross, J. (1993). A nickel metal hydride battery for electric vehicles. Science *260*, 176–181.

Padhi, A.K., Nanjundaswamy, K.S., and Goodenough, J.B. (1997). Phospho-olivines as positive-electrode materials for rechargeable lithium batteries. J. Electrochem. Soc. *144*, 1188–1194.

Panchal, S., Dincer, I., Agelin-Chaab, M., Fraser, R., and Fowler, M. (2017). Transient electrochemical heat transfer modeling and experimental validation of a large sized LiFePO4/graphite battery. Int. J. Heat Mass Transfer. *109*, 1239–1251.

Panchal, S., Mathew, M., Fraser, R., and Fowler, M. (2018). Electrochemical thermal modeling and experimental measurements of 18650 cylindrical lithium-ion battery during discharge cycle for an EV. Appl. Therm. Eng. *135*, 123–132.

Pang, S., Farrell, J., Du, J., and Barth, M. (2001). Battery state-of-charge estimation. In Proceedings of the 2001 American Control Conference. (Cat. No. 01CH37148) (IEEE), pp. 1644–1649.

Park, K., Choi, Y., Choi, W.J., Ryu, H.-Y., and Kim, H. (2020). LSTM-based battery remaining useful life prediction with multi-channel charging profiles. IEEE Access *8*, 20786–20798.

Parker, G. (2001). Encyclopedia of Materials: Science and Technology (Elsevier), http://eprints.soton.ac.uk/id/eprint/259958.

Peters, J.F., Baumann, M., Zimmermann, B., Braun, J., and Weil, M. (2017). The environmental impact of Li-ion batteries and the role of key parameters–A review. Renew. Sustain. Energy Rev. *67*, 491–506.

Placek, M. (2021). Share of the Global Lithium-Ion Battery Manufacturing Capacity in 2020 with a Forecast for 2025, by country [Online]. https://www.statista.com/statistics/1249871/share-of-the-global-lithium-ion-battery-manufacturing-capacity-by-country/.

Poullikkas, A. (2013). A comparative overview of large-scale battery systems for electricity storage. Renew. Sustain. Energy Rev. *27*, 778–788.

Prieto, R., Oliver, J., Reglero, I., and Cobos, J. (2009). Generic battery model based on a parametric implementation. In 2009 Twenty-Fourth Annual IEEE Applied Power Electronics Conference and Exposition (IEEE), pp. 603–607.

Qiao, S., Hu, M., Fu, C., Qin, D., Zhou, A., Wang, P., and Lin, F. (2019). Experimental study on storage and maintenance method of Ni-MH battery modules for hybrid electric vehicles. Appl. Sci. *9*, 1742.

Ramadass, P., Haran, B., White, R., and Popov, B.N. (2002). Capacity fade of Sony 18650 cells cycled at elevated temperatures: part I. Cycling performance. J. Power Sources *112*, 606–613.

Ramadass, P., Haran, B., White, R., and Popov, B.N. (2003). Mathematical modeling of the capacity fade of Li-ion cells. J. Power Sources *123*, 230–240.

Rao, Z., and Wang, S. (2011). A review of power battery thermal energy management. Renew. Sustain. Energy Rev. *15*, 4554–4571. https://doi.org/10.1016/j.rser.2011.07.096.

Ratnakumar, B., Smart, M., and Surampudi, S. (2001). Effects of SEI on the kinetics of lithium intercalation. J. Power Sources *97*, 137–139.

Refino, A.D., Yulianto, N., Syamsu, I., Nugroho, A.P., Hawari, N.H., Syring, A., Kartini, E., Iskandar, F., Voss, T., and Sumboja, A. (2021). Versatilely tuned vertical silicon nanowire arrays by cryogenic reactive ion etching as a lithium-ion battery anode. Sci. Rep. *11*, 1–15.

Ren, L., Zhao, L., Hong, S., Zhao, S., Wang, H., and Zhang, L. (2018). Remaining useful life prediction for lithium-ion battery: a deep learning approach. IEEE Access *6*, 50587–50598.

Richardson, R.R., Osborne, M.A., and Howey, D.A. (2019). Battery health prediction under generalized conditions using a Gaussian process transition model. J. Energy Storage *23*, 320–328.

Robinson, J.B., Darr, J.A., Eastwood, D.S., Hinds, G., Lee, P.D., Shearing, P.R., Taiwo, O.O., and Brett, D.J. (2014). Non-uniform temperature distribution in Li-ion batteries during discharge–a combined thermal imaging, X-ray micro-tomography and electrochemical impedance approach. J. Power Sources *252*, 51–57.

Roth, E.P., Crafts, C.C., Doughty, D.H., and Mcbreen, J. (2004). Advanced technology development program for lithium-ion batteries: thermal abuse performance of 18650 Li-ion cells. Sandia Rep. *584*, 1–139.

Ryu, H., Ahn, H., Kim, K., Ahn, J., Cho, K., and Nam, T. (2006). Self-discharge characteristics of lithium/sulfur batteries using TEGDME liquid electrolyte. Electrochim. Acta *52*, 1563–1566.

Ryu, H., Ahn, H., Kim, K., Ahn, J., Lee, J.-Y., and Cairns, E. (2005). Self-discharge of lithium–sulfur cells using stainless-steel current-collectors. J. Power Sources *140*, 365–369.

Ryu, J., Song, W.J., Lee, S., Choi, S., and Park, S. (2020). A game changer: functional nano/micromaterials for smart rechargeable batteries. Adv. Funct. Mater. *30*, 1902499.

Sabatier, J., Cugnet, M., Laruelle, S., Grugeon, S., Sahut, B., Oustaloup, A., and Tarascon, J. (2010). A fractional order model for lead-acid battery crankability estimation. Commun.Nonlinear Sci. Numer.Simulat. *15*, 1308–1317.

Sabet, P.S., Stahl, G., and Sauer, D.U. (2018). Non-invasive investigation of predominant processes in the impedance spectra of high energy lithium-ion batteries with nickel-cobalt-aluminum cathodes. J. Power Sources *406*, 185–193.

Salameh, Z.M., Casacca, M.A., and Lynch, W.A. (1992). A mathematical model for lead-acid batteries. IEEE Trans. EnergyConvers. *7*, 93–98.

Samaniego, B., Carla, E., O'neill, L., and Nestoridi, M. (2017). High specific energy lithium sulfur cell for space application. In E3S Web of Conferences. EDP Sciences, p. 08006.

Santhanagopalan, S., Zhang, Q., Kumaresan, K., and White, R.E. (2008). Parameter estimation and life modeling of lithium-ion cells. J. Electrochem. Soc. *155*, A345–A353.

Sasaki, T., Ukyo, Y., and Novák, P. (2013). Memory effect in a lithium-ion battery. Nat. Mater. *12*, 569–575.

Sato, Y., Takeuchi, S., and Kobayakawa, K. (2001). Cause of the memory effect observed in alkaline secondary batteries using nickel electrode. J. Power Sources *93*, 20–24.

Saw, L., Ye, Y., and Tay, A. (2013). Electrochemical–thermal analysis of 18650 lithium iron phosphate cell. Energy Convers.Manage. *75*, 162–174.

Scrosati, B., Hassoun, J., and Sun, Y.-K. (2011). Lithium-ion batteries.A look into the future. Energy Environ. Sci. *4*, 3287–3295.

Senthilkumar, M., Tanuja, K., Satyavani, T., Babu, V.R., and Naidu, S. (2017). Effect of temperature and charge stand on electrochemical performance of fiber nickel–cadmium cell. Russ. J. Electrochem. *53*, 161–169.

Seong, W.M., Park, K.-Y., Lee, M.H., Moon, S., Oh, K., Park, H., Lee, S., and Kang, K. (2018). Abnormal self-discharge in lithium-ion batteries. Energy Environ. Sci. *11*, 970–978.

Shi, T., Tu, Q., Tian, Y., Xiao, Y., Miara, L.J., Kononova, O., and Ceder, G. (2020). High active material loading in all-solid-state battery electrode via particle size optimization. Adv. EnergyMater. *10*, 1902881.

Shi, Y., Ahmad, S., Liu, H., Lau, K.T., and Zhao, J. (2021). Optimization of air-cooling technology for LiFePO4 battery pack based on deep learning. J. Power Sources *497*, 229894.

Shim, E.-G., Nam, T.-H., Kim, J.-G., Kim, H.-S., and Moon, S.-I. (2007). Effects of functional electrolyte additives for Li-ion batteries. J. Power Sources *172*, 901–907.

Shim, J., Kostecki, R., Richardson, T., Song, X., and Striebel, K.A. (2002). Electrochemical analysis for cycle performance and capacity fading of a lithium-ion battery cycled at elevated temperature. J. Power Sources *112*, 222–230.

Shu, X., Shen, S., Shen, J., Zhang, Y., Li, G., Chen, Z., and Liu, Y. (2021). State of health prediction of lithium-ion batteries based on machine learning: advances and perspectives. iScience *24*, 103265.

Singh, R., Polu, A.R., Bhattacharya, B., Rhee, H.-W., Varlikli, C., and Singh, P.K. (2016). Perspectives for solid biopolymer electrolytes in dye sensitized solar cell and battery application. Renew. Sustain. Energy Rev. *65*, 1098–1117.

Singhal, R., Das, S.R., Oviedo, O., Tomar, M.S., and Katiyar, R.S. (2006). Improved electrochemical properties of a coin cell using LiMn1.5Ni0. 5O4 as cathode in the 5 V range. J. Power Sources *160*, 651–656.

Sloop, S.E., Kerr, J.B., and Kinoshita, K. (2003). The role of Li-ion battery electrolyte reactivity in performance decline and self-discharge. J. Power Sources *119*, 330–337.

Smart, M., Ratnakumar, B., and Surampudi, S. (1999). Electrolytes for low-temperature lithium batteries based on ternary mixtures of aliphatic carbonates. J. Electrochem. Soc. *146*, 486.

Smart, M., Ratnakumar, B., Whitcanack, L., Chin, K., Rodriguez, M., and Surampudi, S. (2002). Performance characteristics of lithium ion cells at low temperatures. IEEE Aerospace Electron. Syst. Mag. *17*, 16–20.

Smart, M., Ratnakumar, B., Whitcanack, L., Chin, K., Surampudi, S., Croft, H., Tice, D., and Staniewicz, R. (2003). Improved low-temperature performance of lithium-ion cells with quaternary carbonate-based electrolytes. J. Power Sources *119*, 349–358.

Smith, K., Kim, G.H., Darcy, E., and Pesaran, A. (2010). Thermal/electrical modeling for abuse-tolerant design of lithium ion modules. Int. J. Energy Res. *34*, 204–215.

Somasundaram, K., Birgersson, E., and Mujumdar, A.S. (2012). Thermal–electrochemical model for passive thermal management of a spiral-wound lithium-ion battery. J. Power Sources *203*, 84–96.

Song, J., Wang, Y., and Wan, C.C. (1999). Review of gel-type polymer electrolytes for lithium-ion batteries. J. Power Sources *77*, 183–197.

Song, S., Yu, L., Ruan, Y., Sun, J., Chen, B., Xu, W., and Zhang, J.-G. (2019). Highly efficient Ru/B4C multifunctional oxygen electrode for rechargeable LiO2 batteries. J. Power Sources *413*, 11–19.

Song, W.-J., Lee, S., Song, G., Son, H.B., Han, D.-Y., Jeong, I., Bang, Y., and Park, S. (2020). Recent progress in aqueous based flexible energy storage devices. Energy Storage Mater. *30*, 260–286.

Spotnitz, R., and Franklin, J. (2003). Abuse behavior of high-power, lithium-ion cells. J. Power Sources *113*, 81–100.

Stambouli, A.B. (2011). Fuel cells: the expectations for an environmental-friendly and sustainable source of energy. Renew. Sustain. Energy Rev. *15*, 4507–4520.

Stephan, A.M. (2006). Review on gel polymer electrolytes for lithium batteries. Eur. Polym. J. *42*, 21–42.

Stroe, D.-I., Swierczynski, M., Kær, S.K., and Teodorescu, R. (2017). Degradation behavior of lithium-ion batteries during calendar ageing—the case of the internal resistance increase. IEEE Trans. Ind. Appl. *54*, 517–525.

Stroe, D.-I., Swierczynski, M., and Teodorescu, R. (2016). A comprehensive study on the degradation of lithium-ion batteries during calendar ageing: the internal resistance increase. In 2016 IEEE Energy Conversion Congress and Exposition (ECCE) (IEEE), pp. 1–7.

Suberu, M.Y., Mustafa, M.W., and Bashir, N. (2014). Energy storage systems for renewable energy power sector integration and mitigation of intermittency. Renew. Sustain. Energy Rev. *35*, 499–514.

Sujitha, N., and Krithiga, S. (2017). RES based EV battery charging system: a review. Renew. Sustain. Energy Rev. *75*, 978–988.

Sun, L., Li, G., and You, F. (2020a). Combined internal resistance and state-of-charge estimation of lithium-ion battery based on extended state observer. Renew. Sustain. Energy Rev. *131*, 109994.

Sun, W., Suo, L., Wang, F., Eidson, N., Yang, C., Han, F., Ma, Z., Gao, T., Zhu, M., and Wang, C. (2017). "Water-in-Salt" electrolyte enabled LiMn2O4/TiS2 Lithium-ion batteries. Electrochem.Commun. *82*, 71–74.

Sun, X., Li, Z., Wang, X., and Li, C. (2020b). Technology development of electric vehicles: a review. Energies *13*, 90.

Sun, Y., Hao, X., Pecht, M., and Zhou, Y. (2018). Remaining useful life prediction for lithium-ion batteries based on an integrated health indicator. Microelectron.Reliab. *88*, 1189–1194.

Suo, L., Borodin, O., Gao, T., Olguin, M., Ho, J., Fan, X., Luo, C., Wang, C., and Xu, K. (2015). "Water-in-salt" electrolyte enables high-voltage aqueous lithium-ion chemistries. Science *350*, 938–943.

Swierczynski, M., Stroe, D.-I., Stan, A.-I., Teodorescu, R., and Kær, S.K. (2014). Investigation on the self-discharge of the LiFePO 4/C nanophosphate battery chemistry at different conditions. In 2014 IEEE Conference and Expo Transportation Electrification Asia-Pacific (ITEC Asia-Pacific) (IEEE), pp. 1–6.

Tan, L., Zhang, L., Sun, Q., Shen, M., Qu, Q., and Zheng, H. (2013). Capacity loss induced by lithium deposition at graphite anode for LiFePO4/graphite cell cycling at different temperatures. Electrochim. Acta *111*, 802–808.

Tan, X., Tan, Y., Zhan, D., Yu, Z., Fan, Y., Qiu, J., and Li, J. (2020). Real-time state-of-health estimation of lithium-ion batteries based on the equivalent internal resistance. IEEE Access *8*, 56811–56822.

Tarascon, J., Mckinnon, W., Coowar, F., Bowmer, T., Amatucci, G., and Guyomard, D. (1994). Synthesis conditions and oxygen stoichiometry effects on Li insertion into the spinel LiMn2 O 4. J. Electrochem. Soc. *141*, 1421–1431.

Thomas, K.E., and Newman, J. (2003). Thermal modeling of porous insertion electrodes. J. Electrochem. Soc. *150*, A176–A192.

Tie, S.F., and Tan, C.W. (2013). A review of energy sources and energy management system in electric vehicles. Renew. Sustain. Energ. Rev. *20*, 82–102.

Tourani, A., White, P., and Ivey, P. (2014). A multi scale multi-dimensional thermo electrochemical modelling of high capacity lithium-ion cells. J. Power Sources *255*, 360–367.

Tremblay, O., Dessaint, L.-A., and Dekkiche, A.-I. (2007). A generic battery model for the dynamic simulation of hybrid electric vehicles. In 2007 IEEE Vehicle Power and Propulsion Conference (IEEE), pp. 284–289.

Turetskyy, A., Thiede, S., Thomitzek, M., Von Drachenfels, N., Pape, T., and Herrmann, C. (2020). Toward data-driven applications in lithium-ion battery cell manufacturing. EnergyTechnol. *8*, 1900136.

Ulldemolins, M., Le Cras, F., and Pecquenard, B. (2013). Memory effect highlighting in silicon anodes for high energy density lithium-ion batteries. Electrochem.Commun. *27*, 22–25.

Ulrich, L. (2019). Top ten tech cars 2019: self-driving and electric technologies are infiltrating everyday cars—slowly. IEEE Spectr. *56*, 32–43.

Vaalma, C., Buchholz, D., Weil, M., and Passerini, S. (2018). A cost and resource analysis of sodium-ion batteries. Nat. Rev. Mater. *3*, 1–11.

Vazquez-Arenas, J., Gimenez, L.E., Fowler, M., Han, T., and Chen, S.-K. (2014). A rapid estimation and sensitivity analysis of parameters describing the behavior of commercial Li-ion batteries

including thermal analysis. Energy Convers.Manage. *87*, 472–482.

Verma, P., Maire, P., and Novak, P. (2010). Electrochim.Acta *55*, 6332.

Vetter, J., Novák, P., Wagner, M.R., Veit, C., Möller, K.-C., Besenhard, J., Winter, M., Wohlfahrt-Mehrens, M., Vogler, C., and Hammouche, A. (2005). Ageing mechanisms in lithium-ion batteries. J. Power Sources *147*, 269–281.

Krause, F., Bugga, R., Billings, K., Ruiz, J.P., Brandon, E., Darcy, E., and Iannello, C. (2019). Commercial 18650 lithium-ion cells for high-energy, high-power, and radiation applications. 36th Meeting of the Electrochemical Society, Atlanta, GA, October 15, 2019 . https://trs.jpl.nasa.gov/bitstream/handle/2014/51890/CL%2319-6583.pdf?sequence=1.

Vieira, E.M., Ribeiro, J.F., Sousa, R., Rolo, A.G., Silva, M.M., and Goncalves, L.M. (2017). Flexible solid-state Ge–LiCoO2 battery: from materials to device application. Advanced Materials Letters. https://www.researchgate.net/profile/J-Ribeiro-2/publication/317926892_Flexible_Solid-State_Ge_-_LiCoO2_Battery_From_Materials_To_Device_Application/links/59a3eadd458515703116f7f8/Flexible-Solid-State-Ge-LiCoO2-Battery-From-Materials-To-Device-Application.pdf.

Waldmann, T., Wilka, M., Kasper, M., Fleischhammer, M., and Wohlfahrt-Mehrens, M. (2014). Temperature dependent ageing mechanisms in lithium-ion batteries–a post-mortem study. J. Power Sources *262*, 129–135.

Wan, Z., Lei, D., Yang, W., Liu, C., Shi, K., Hao, X., Shen, L., Lv, W., Li, B., and Yang, Q.H. (2019). Low resistance–integrated all-solid-state battery achieved by Li7La3Zr2O12 nanowire upgrading polyethylene oxide (PEO) composite electrolyte and PEO cathode binder. Adv. Funct. Mater. *29*, 1805301.

Wang, C., Lin, T., Huang, J., and Rao, Z. (2015). Temperature response of a high power lithium-ion battery subjected to high current discharge. Mater. Res. Innov. *19*, S2-156-S2-160.

Wang, C., Zhang, G., Meng, L., Li, X., Situ, W., Lv, Y., and Rao, M. (2017a). Liquid cooling based on thermal silica plate for battery thermal management system. Int. J. Energy Res. *41*, 2468–2479.

Wang, D., Yang, F., Zhao, Y., and Tsui, K.-L. (2017b). Battery remaining useful life prediction at different discharge rates. Microelectron.Reliab. *78*, 212–219.

Wang, H., Liang, Y., Gong, M., Li, Y., Chang, W., Mefford, T., Zhou, J., Wang, J., Regier, T., and Wei, F. (2012a). An ultrafast nickel–iron battery from strongly coupled inorganic nanoparticle/nanocarbon hybrid materials. Nat. Commun. *3*, 1–8.

Wang, H., Tao, T., Xu, J., Mei, X., Liu, X., and Gou, P. (2020a). Cooling capacity of a novel modular liquid-cooled battery thermal management system for cylindrical lithium ion batteries. Appl. Therm. Eng. *178*, 115591.

Wang, Q., Jiang, B., Li, B., and Yan, Y. (2016). A critical review of thermal management models and solutions of lithium-ion batteries for the development of pure electric vehicles. Renew. Sustain. Energy Rev. *64*, 106–128. https://doi.org/10.1016/j.rser.2016.05.033.

Wang, Q., Ping, P., Zhao, X., Chu, G., Sun, J., and Chen, C. (2012b). Thermal runaway caused fire and explosion of lithium ion battery. J. Power Sources *208*, 210–224.

Wang, Q., Sun, J., Yao, X., and Chen, C. (2006). Thermal behavior of lithiated graphite with electrolyte in lithium-ion batteries. J. Electrochem. Soc. *153*, A329–A333.

Wang, S., Fernandez, C., Yu, C., Fan, Y., Cao, W., and Stroe, D.-I. (2020b). A novel charged state prediction method of the lithium ion battery packs based on the composite equivalent modeling and improved splice Kalman filtering algorithm. J. Power Sources *471*, 228450.

Wang, Z., Sun, Z., Shi, Y., Qi, F., Gao, X., Yang, H., Cheng, H.M., and Li, F. (2021). Ion-dipole chemistry drives rapid evolution of Li ions solvation sheath in low-temperature Li batteries. Adv. EnergyMater. *11*, 2100935.

Wegmann, R., Döge, V., and Sauer, D.U. (2018). Assessing the potential of an electric vehicle hybrid battery system comprising solid-state lithium metal polymer high energy and lithium-ion high power batteries. J. Energy Storage *18*, 175–184.

Wei, J., Chen, B., Su, H., Jiang, C., Li, X., Qiao, S., and Zhang, H. (2021). Co9S8 nanotube wrapped with graphene oxide as sulfur hosts with ultra-high sulfur content for lithium-sulfur battery. Ceramics Int. *47*, 2686–2693.

Wei, J., Dong, G., and Chen, Z. (2017). Remaining useful life prediction and state of health diagnosis for lithium-ion batteries using particle filter and support vector regression. IEEE Trans. Ind. Electron. *65*, 5634–5643.

Wei, S., Xu, S., Agrawral, A., Choudhury, S., Lu, Y., Tu, Z., Ma, L., and Archer, L.A. (2016). A stable room-temperature sodium–sulfur battery. Nat. Commun. *7*, 11722.

Wei, X., Zhu, B., and Xu, W. (2009). Internal resistance identification in vehicle power lithium-ion battery and application in lifetime evaluation. In 2009 International Conference on Measuring Technology and Mechatronics Automation (IEEE), pp. 388–392.

Wen, G., Rehman, S., Tranter, T.G., Ghosh, D., Chen, Z., Gostick, J.T., and Pope, M.A. (2020). Insights into multiphase reactions during self-discharge of Li-S batteries. Chem. Mater. *32*, 4518–4526.

Widanage, W., Barai, A., Chouchelamane, G., Uddin, K., Mcgordon, A., Marco, J., and Jennings, P. (2016). Design and use of multisine signals for Li-ion battery equivalent circuit modelling. Part 1: signal design. J. Power Sources *324*, 70–78.

Williamson, S.S., Rimmalapudi, S.C., and Emadi, A. (2004). Electrical modeling of renewable energy sources and energy storage devices. J. Power Electron. *4*, 117–126.

Wisniewski, D. (2010). Solar flair: an open-road challenge. IEEE Potentials *29*, 6–9.

Wood, D.L., III, Li, J., and An, S.J. (2019). Formation challenges of lithium-ion battery manufacturing. Joule *3*, 2884–2888.

Wright, R., Christophersen, J., Motloch, C., Belt, J., Ho, C., Battaglia, V., Barnes, J., Duong, T., and Sutula, R. (2003). Power fade and capacity fade resulting from cycle-life testing of advanced technology development program lithium-ion batteries. J. Power Sources *119*, 865–869.

Wu, W., Wu, W., and Wang, S. (2018). Thermal management optimization of a prismatic battery with shape-stabilized phase change material. Int. J. Heat Mass Transfer. *121*, 967–977.

Wu, X.-L., Guo, Y.-G., Su, J., Xiong, J.-W., Zhang, Y.-L., and Wan, L.-J. (2013). Carbon-nanotube-decorated nano-LiFePO4 @C cathode material with superior high-rate and low-temperature performances for lithium-ion batteries. Adv. EnergyMater. *3*, 1155–1160. https://doi.org/10.1002/aenm.201300159.

Wu, Y., Keil, P., Schuster, S.F., and Jossen, A. (2017). Impact of temperature and discharge rate on the aging of a LiCoO2/LiNi0.8Co0. 15Al0. 05O2 lithium-ion pouch cell. J. Electrochem. Soc. *164*, A1438–A1445.

Xia, C., Guo, J., Lei, Y., Liang, H., Zhao, C., and Alshareef, H.N. (2018). Rechargeable aqueous zinc-ion battery based on porous framework zinc pyrovanadate intercalation cathode. Adv. Mater. *30*, 1705580.

Xiao, J., Chernova, N.A., and Whittingham, M.S. (2010). Influence of manganese content on the performance of LiNi0. 9− y Mn y Co0.1O2 (0.45≤ y≤ 0.60) as a cathode material for Li-ion batteries. Chem. Mater. *22*, 1180–1185.

Xiong, R. (2020). Remaining useful life prediction of lithium-ion batteries. Battery Management Algorithm for Electric Vehicles (Springer Singapore), pp. 217–242.

Xiong, R., Li, L., and Tian, J. (2018). Towards a smarter battery management system: a critical review on battery state of health monitoring methods. J. Power Sources *405*, 18–29.

Xiong, R., Ma, S., Li, H., Sun, F., and Li, J. (2020). Toward a safer battery management system: a critical review on diagnosis and prognosis of battery short circuit. Iscience *23*, 101010.

Xu, C., Wu, L., Hu, S., Xie, H., and Zhang, X. (2019). A heavily surface-doped polymer with the bifunctional catalytic mechanism in Li-O2 batteries. Iscience *14*, 312–322.

Xu, F., Yang, F., Fei, Z., Huang, Z., and Tsui, K.-L. (2021). Life prediction of lithium-ion batteries based on stacked denoising autoencoders. Reliab. Eng. Syst. Saf. *208*, 107396.

Xu, K. (2004). Nonaqueous liquid electrolytes for lithium-based rechargeable batteries. Chem. Rev. *104*, 4303–4418.

Xu, Z., Wang, T., Kong, L., Yao, K., Fu, H., Li, K., Cao, L., Huang, J., and Zhang, Q. (2017). MoO2@MoS2 nanoarchitectures for high-loading advanced lithium-ion battery anodes. Part. Part. Syst. Char. *34*, 1600223.

Yaakov, D., Gofer, Y., Aurbach, D., and Halalay, I.C. (2010). On the study of electrolyte solutions

for Li-ion batteries that can work over a wide temperature range. J. Electrochem. Soc. *157*, A1383–A1391.

Yamauchi, H., Ikejiri, J., Tsunoda, K., Tanaka, A., Sato, F., Honma, T., and Komatsu, T. (2020). Enhanced rate capabilities in a glass-ceramic-derived sodium all-solid-state battery. Sci. Rep. *10*, 1–12.

Yang, H., Chen, X., Yao, N., Piao, N., Wang, Z., He, K., Cheng, H.-M., and Li, F. (2021a). Dissolution–precipitation dynamics in ester electrolyte for high-stability lithium metal batteries. ACS EnergyLett. *6*, 1413–1421.

Yang, T., Gao, W., Guo, B., Zhan, R., Xu, Q., He, H., Bao, S.-J., Li, X., Chen, Y., and Xu, M. (2019). A railway-like network electrode design for room temperature Na–S battery. J. Mater. Chem. A *7*, 150–156.

Yang, W., Zhou, F., Chen, X., and Zhang, Y. (2021b). Performance analysis of axial air cooling system with shark-skin bionic structure containing phase change material. Energy Convers.Manage. *250*, 114921.

Yang, X.-G., Liu, T., and Wang, C.-Y. (2021c). Thermally modulated lithium iron phosphate batteries for mass-market electric vehicles. Nat. Energy *6*, 176–185.

Yang, Y., Hu, X., Qing, D., and Chen, F. (2013). Arrhenius equation-based cell-health assessment: application to thermal energy management design of a HEV NiMH battery pack. Energies *6*, 2709–2725.

Yang, Y., Mcdowell, M.T., Jackson, A., Cha, J.J., Hong, S.S., and Cui, Y. (2010). New nanostructured Li2S/silicon rechargeable battery with high specific energy. Nano Lett. *10*, 1486–1491.

Yao, L.W., Aziz, J., Kong, P.Y., Idris, N., and Alsofyani, I. (2014). Modeling of lithium titanate battery for charger design. In 2014 Australasian Universities Power Engineering Conference (AUPEC) (IEEE), pp. 1–5.

Yao, M., Gan, Y., Liang, J., Dong, D., Ma, L., Liu, J., Luo, Q., and Li, Y. (2021). Performance simulation of a heat pipe and refrigerant-based lithium-ion battery thermal management system coupled with electric vehicle air-conditioning. Appl. Therm. Eng. *191*, 116878.

Yatabe, K., Horiba, T., Kubota, K., Fukunishi, M., Yabuuchi, N., Oji, H., Son, J.-Y., Cui, Y.-T., Yasuno, S., and Komaba, S. (2018). Effect of diphenylethane as an electrolyte additive to enhance high-temperature durability of LiCoO2/graphite cells. Electrochim. Acta *270*, 120–128.

Ye, Y., Saw, L.H., Shi, Y., Somasundaram, K., and Tay, A.A. (2014). Effect of thermal contact resistances on fast charging of large format lithium ion batteries. Electrochim. Acta *134*, 327–337.

Yoshida, H., Imamura, N., Inoue, T., and Komada, K. (2003). Capacity loss mechanism of space lithium-ion cells and its life estimation method. Electrochemistry *71*, 1018–1024.

Yoshida, T., Takahashi, M., Morikawa, S., Ihara, C., Katsukawa, H., Shiratsuchi, T., and Yamaki, J.-I. (2006). Degradation mechanism and life prediction of lithium-ion batteries. J. Electrochem. Soc. *153*, A576–A582.

Young, K.-H. (2018). Research in Nickel/Metal Hydride Batteries 2017 (Multidisciplinary Digital Publishing Institute).

Young, K., Wang, C., and Strunz, K. (2013). Electric vehicle battery technologies. In Electric Vehicle Integration into Modern Power Networks (Springer), pp. 15–56.

Yu, C., Chen, X., Xiao, Z., Lei, C., Zhang, C., Lin, X., Shen, B., Zhang, R., and Wei, F. (2019). Silicon carbide as a protective layer to stabilize Si-based anodes by inhibiting chemical reactions. Nano Lett. *19*, 5124–5132.

Yuan, L., Feng, J., Ai, X., Cao, Y., Chen, S., and Yang, H. (2006). Improved dischargeability and reversibility of sulfur cathode in a novel ionic liquid electrolyte. Electrochem.Commun. *8*, 610–614.

Yuan, T., Yu, X., Cai, R., Zhou, Y., and Shao, Z. (2010). Synthesis of pristine and carbon-coated Li4Ti5O12 and their low-temperature electrochemical performance. J. Power Sources *195*, 4997–5004.

Yuan, X., Razzaq, A.A., Chen, Y., Lian, Y., Zhao, X., Peng, Y., and Deng, Z. (2021). Polyacrylonitrile-based gel polymer electrolyte filled with Prussian blue forhigh-performance lithium polymer batteries. Chin. Chem. Lett. *32*, 890–894.

Yue, L.. https://koara.lib.keio.ac.jp/xoonips/modules/xoonips/download.php/KO40003001-00002020-3700.pdf?file_id=160665.

Zelinsky, M.A., Koch, J.M., and Young, K.-H. (2018). Performance comparison of rechargeable batteries for stationary applications (Ni/MH vs. Ni–Cd and VRLA). Batteries *4*, 1.

Zeng, G., An, Y., Xiong, S., and Feng, J. (2019a). Nonflammable fluorinated carbonate electrolyte with high salt-to-solvent ratios enables stable silicon-based anode for next-generation lithium-ion batteries. ACS Appl. Mater. Inter. *11*, 23229–23235.

Zeng, X., Li, J., and Liu, L. (2015). Solving spent lithium-ion battery problems in China: opportunities and challenges. Renew. Sustain. Energy Rev. *52*, 1759–1767.

Zeng, X., Li, M., Abd El-Hady, D., Alshitari, W., Al-Bogami, A.S., Lu, J., and Amine, K. (2019b). Commercialization of lithium battery technologies for electric vehicles. Adv. EnergyMater. *9*, 1900161.

Zhang, H., and Chow, M.-Y. (2010). Comprehensive dynamic battery modeling for PHEV applications. In IEEE PES General Meeting (IEEE), pp. 1–6.

Zhang, S., Pollard, T.P., Feng, X., Borodin, O., Xu, K., and Li, Z. (2020a). Altering the electrochemical pathway of sulfur chemistry with oxygen for high energy density and low shuttling in a Na/S battery. ACS EnergyLett. *5*, 1070–1076.

Zhang, S., Xu, K., Allen, J., and Jow, T. (2002a). Effect of propylene carbonate on the low temperature performance of Li-ion cells. J. Power Sources *110*, 216–221.

Zhang, S., Xu, K., and Jow, T. (2002b). Low temperature performance of graphite electrode in Li-ion cells. Electrochim. Acta *48*, 241–246.

Zhang, S., Xu, K., and Jow, T. (2002c). A new approach toward improved low temperature performance of Li-ion battery. Electrochem.Commun. *4*, 928–932.

Zhang, S., Xu, K., and Jow, T. (2003). The low temperature performance of Li-ion batteries. J. Power Sources *115*, 137–140.

Zhang, S., Xu, K., and Jow, T. (2004). Electrochemical impedance study on the low temperature of Li-ion batteries. Electrochim. Acta *49*, 1057–1061.

Zhang, S.S. (2006). A review on electrolyte additives for lithium-ion batteries. J. Power Sources *162*, 1379–1394.

Zhang, X., Lu, J., Yuan, S., Yang, J., and Zhou, X. (2017a). A novel method for identification of lithium-ion battery equivalent circuit model parameters considering electrochemical properties. J. Power Sources *345*, 21–29.

Zhang, X., Miao, Q., and Liu, Z. (2017b). Remaining useful life prediction of lithium-ion battery using an improved UPF method based on MCMC. Microelectron.Reliab. *75*, 288–295.

Zhang, Y., Wan, F., Huang, S., Wang, S., Niu, Z., and Chen, J. (2020b). A chemically self-charging aqueous zinc-ion battery. Nat. Commun. *11*, 1–10.

Zhao, G., Wang, X., and Negnevitsky, M. (2021a). A study of variable cell spacings to the heat transfer efficiency of air-cooling battery thermal management system. Appl. Sci. *11*, 11155.

Zhao, G., Wang, X., Negnevitsky, M., and Zhang, H. (2021b). A review of air-cooling battery thermal management systems for electric and hybrid electric vehicles. J. Power Sources *501*, 230001.

Zhao, J., Xue, F., Fu, Y., Cheng, Y., Yang, H., and Lu, S. (2021c). A comparative study on the thermal runaway inhibition of 18650 lithium-ion batteries by different fire extinguishing agents. Iscience *24*, 102854.

Zhao, R., Zhang, S., Liu, J., and Gu, J. (2015). A review of thermal performance improving methods of lithium ion battery: electrode modification and thermal management system. J. Power Sources *299*, 557–577. https://doi.org/10.1016/j.jpowsour.2015.09.001.

Zhao, T., Zhu, D., Li, W., Li, A., and Zhang, J. (2019). Novel design and synthesis of carbon-coated porous silicon particles as high-performance lithium-ion battery anodes. J. Power Sources *439*, 227027.

Zheng, Y., He, Y.-B., Qian, K., Liu, D., Lu, Q., Li, B., Wang, X., Li, J., and Kang, F. (2017). Influence of charge rate on the cycling degradation of LiFePO4/mesocarbon microbead batteries under low temperature. Ionics *23*, 1967–1978.

Zhou, W., Li, Y., Xin, S., and Goodenough, J.B. (2017). Rechargeable sodium all-solid-state battery. ACS Cent. Sci. *3*, 52–57.

Zhu, W.H., Zhu, Y., Davis, Z., and Tatarchuk, B.J. (2013). Energy efficiency and capacity retention of Ni–MH batteries for storage applications. Appl. Energy *106*, 307–313.

Zhu, Z., Tang, Y., Lv, Z., Wei, J., Zhang, Y., Wang, R., Zhang, W., Xia, H., Ge, M., and Chen, X. (2018). Fluoroethylene carbonate enabling a robust LiF-rich solid electrolyte interphase to enhance the stability of the MoS2 anode for lithium-ion storage. Angew. Chem. Int. Ed. *57*, 3656–3660.

Zou, C., Zhang, L., Hu, X., Wang, Z., Wik, T., and Pecht, M. (2018). A review of fractional-order techniques applied to lithium-ion batteries, lead-acid batteries, and supercapacitors. J. Power Sources *390*, 286–296.

Zimmerman, A. (2012). Self-discharge losses in lithium ion battery cells. In: 1st International Energy Conversion Engineering Conference (IECEC). American Institute of Aeronautics and Astronautics, 5985.

Zou, P., Sui, Y., Zhan, H., Wang, C., Xin, H.L., Cheng, H.-M., Kang, F., and Yang, C. (2021). Polymorph evolution mechanisms and regulation strategies of lithium metal anode under multiphysical fields. Chem. Rev. *121*, 5986–6056.

Zubi, G., Dufo-López, R., Carvalho, M., and Pasaoglu, G. (2018). The lithium-ion battery: state of the art and future perspectives. Renew. Sustain. Energy Rev. *89*, 292–308.